MODELING COVID-19 SPREAD USING AN AGENT-BASED NETWORK

A Thesis

presented to

the Faculty of California Polytechnic State University,

San Luis Obispo

In Partial Fulfillment

of the Requirements for the Degree

Master of Science in Computer Science

by

Stephen Hung

June 2021

COMMITTEE MEMBERSHIP

TITLE: Modeling COVID-19 Spread Using an Agent-Based Network

AUTHOR: Stephen Hung

DATE SUBMITTED: June 2021

COMMITTEE CHAIR: Theresa Migler, Ph.D.
Assistant Professor of Computer Science

COMMITTEE MEMBER: Franz Kurfess, Ph.D.
Professor of Computer Science

COMMITTEE MEMBER: Paul Anderson, Ph.D.
Associate Professor of Computer Science

COMMITTEE MEMBER: Christopher Siu, M.S.
Lecturer of Computer Science

ABSTRACT

Modeling COVID-19 Spread Using an Agent-Based Network

Stephen Hung

Beginning in 2019 and quickly spreading internationally, the Coronavirus disease Covid-19 became the first pandemic that many people have witnessed firsthand along with the severe disruption to their daily lives. A key field of research for Covid-19 that is studied by epidemiologists, biologists, and computer scientists alike is modeling the spread of Covid-19 in order to better predict future outbreaks of the pandemic and evaluate potential strategies to reduce infections, hospitalizations, and deaths.

This thesis proposes a method of modeling Covid-19 spread and interventions for local environments based on different levels of perspective. The goal for this thesis is to be able to present a model of Covid-19 in terms of surrounding areas in San Luis Obispo including the unique mobility dynamic currently held in the global pandemic. Furthermore, we use our model to explore different methods of ensuring a low infection rate such as isolation methods and mobility restrictions.

ACKNOWLEDGMENTS

Thanks to:

- My family for their extensive support and encouragement throughout my degrees
- Mandy Xu, for your constant support and always believing in me
- Theresa Migler, for being a great advisor and with your encouragement and advice this thesis was made possible
- My friends, for all your support and great times together
- My committee, for all the help and time helping me make this thesis better
- Andrew Guenther, for uploading this template

TABLE OF CONTENTS

LIST OF TABLES

LIST OF FIGURES

Chapter 1

INTRODUCTION

Covid-19 began in December of 2019 when the Wuhan Municipal Health Commission in China reported cases of pneumonia from unknown causes to the World Health Organization (WHO) [38]. Beginning in January 2020, the Wuhan Province fell under quarantine and cases of the new novel coronavirus, Covid-19, were confirmed internationally in the United States, Taiwan, and Hong Kong. By February 2020, many more countries such as India, Italy, the United Kingdom, and more confirmed their first cases of Covid-19 and initiated travel bans to and from China. By the end of February, 56 countries confirmed approximately 84,000 cases and 2,874 cases were reported globally [29]. By March 11 2020, the WHO officially characterized Covid-19 as a pandemic which is defined as "an outbreak of a disease that occurs over a wide geographic area (such as multiple countries or continents) and typically affects a significant proportion of the population" by the Merriam-Webster dictionary [2][36]. In the coming months, countries started instating quarantine measures, all residents were ordered to stay at home, country borders were sealed, in-person schools were closed, and many businesses had to shut down.

However even as many people's daily lives grinded to a halt, scientists, doctors, and many researchers banded together to start analyzing Covid-19's genetic code in order to develop treatments, vaccines, and a deeper understanding of the coronavirus' structure. In a parallel process, researchers from all around the world and from fields ranging from mathematics to epidemiology began researching the spread of Covid-19. They developed models to understand the spread of Covid-19 and help inform policies that governments or businesses would develop. These models included modelling

interventions methods and methods to reduce the hospitalization rate of individuals. As part of the modelling, researchers explored many different factors that were not present in previous pandemics. My thesis focuses on the modelling of such factors in an agent-based contact network for San Luis Obispo specifically and explores intervention methods and their resulting effects.

Chapter 2

BACKGROUND

Infectious diseases have been present in mankind's history for almost as long as our written history. Signs of rabies, a disease that still exists today, were present back in 2300 B.C. where Babylonian laws dictated that if a dog transmitted rabies, the owner would have to pay a fine [21]. In comparison to the age of infectious diseases, the study of infectious diseases and their spread is a relatively younger field. John Graunt is regarded as one of the first epidemiologists, scientists who study infectious diseases, when he published the 1662 book "Natural and Political Observations made upon the Bills of Mortality" which related human diseases and the ensuing deaths [15]. The foundation for modern infectious disease models can be drawn from the Kermack–McKendrick & Reed–Frost epidemic models which emerged in the 1920s and related susceptible, infected, and immune (recovered) population models [30][3]. Kermack-McKendrick's model was able to predict epidemic behavior similar to previously recorded epidemics and is the foundation for what will come to be known as a compartmental model.

2.1 Coronaviruses

Although Covid-19 is often referred to as "the coronavirus" colloquially, Covid-19 is in fact only one of many coronaviruses [44]. The coronavirus that is causing the current pandemic, Covid-19, is known as SARS-CoV-2 which stands for Severe Acute Respiratory Syndrome Coronavirus 2 and is the second virus very similar to SARS [8]. SARS is a disease caused by the coronavirus SARS-CoV-1 which resulted in the

2002-2004 SARS outbreak. In comparison to Covid-19, SARS was relatively smaller in scope as it infected a total of 8,422 individuals with a fatality rate of 11% by the end of the epidemic. Both disease share very similar symptoms such as fever, headaches, and respiratory symptoms like coughing.

Coronaviruses are a family of viruses that are commonly seen in birds and mammals with differing effects [33]. Coronaviruses are named as such because the virus' outer surface has short spiky protrusions similar to a crown (translated to corona in Latin). Coronaviruses contain spike proteins which allow the virus to penetrate certain cells in the body and offload its' viral load thereby turning the infected cell into a virus producing cell. Originally coronaviruses were native to animals but over time evolved to infect humans too. SARS for instance was found to occur from civets while MERS was found to be from camels. While Covid-19's animal precursor has not been found yet, bats have been identified as one of the possible precursors to an intermediate carrier which then infected humans. Coronaviruses are also not a relatively new occurrence as the first human coronavirus was identified in the mid-1960s [9]. There are four common strains of coronaviruses which cause the common cold in human individuals. These four common strains are referred to as:

- 229E (alpha coronavirus)
- NL63 (alpha coronavirus)
- OC43 (beta coronavirus)
- HKU1 (beta coronavirus)

229E and OC43 have been found to account for 4-15% of colds annually and a maximum of 35% during peak seasons [40].

Similarities among the coronavirus family includes the high infectiousness and relatively lower fatality rate. SARS had a mortality rate of about 9.6%, Covid-19 is estimated at 2%, and MERS between 30-40%.

In general, coronaviruses are spread by respiratory droplets caused by infected individuals breathing, coughing, or sneezing. Upon infection, human individuals may display mild to severe symptoms similar to a flu but exact symptoms are dependent on the coronavirus.

Coronaviruses can be diagnosed by analyzing blood and respiratory samples. As with colds, there are no treatments that can completely cure the coronavirus and thus individuals usually recover on their own. Vaccines are effective in reducing the spread of coronaviruses. For Covid-19, the first vaccines began rolling out in December of 2020 and will continue throughout 2021 [37].

2.2 Compartmental Models

Compartmental models are mathematical models where the population in the model is split into different labelled compartments. In Kermack-McKendrick's case the compartments were labeled as SIR which stand for

- Susceptible: Individuals who can catch the disease
- Infected: Individuals who currently have the disease and can transmit it
- Recovered/Removed: Individuals who have had the disease and are now immune to it (Individuals that pass away as a result of the disease may also fall into this category as "Removed")

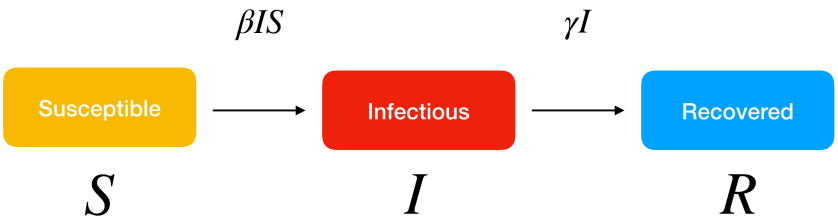

Figure 2.1: Flow of the SIR compartmental model [43]

The order of the labels usually dictates the linear flow of the population so in this case the population flows from Susceptible to Infected and finally to Recovered. This can be seen in Figure 2.1. In order to transition from one compartment to another, differential equations with respect to time are used to represent each compartment. The reason why these equations are with respect to time is because these epidemic models are used to represent the change in epidemic spread over time. An example of these equations for a simple SIR compartmental model is the following [25]:

$$\begin{aligned} \frac{dS}{dt} &= \frac{-\beta IS}{N}, & S(0) &= S_0 \geq 0 \\ \frac{dI}{dt} &= \frac{\beta IS}{N} - \gamma I, & I(0) &= I_0 \geq 0 \\ \frac{dR}{dt} &= \gamma I, & R(0) &= R_0 \geq 0 \end{aligned}$$

Where S, I, and R are shortform for $S(t)$, $I(t)$, $R(t)$ which stands for their respective populations at time t. Given a population N, $S(t)+I(t)+R(t) = N$. β is the contact rate between individuals and $\frac{1}{\gamma}$ is the average infectious period. γI has been shown to correspond to $P(t) = e^{-\gamma t}$ which is the fraction of individuals in the Infective compartment after some time t.

$$\frac{dS}{dt} = \frac{-\beta IS}{N}, \qquad S(0) = S_0 \geq 0$$

The differential equation for the Susceptible population states that the change in population is the proportion of susceptible individuals coming into contact with infected individuals. As the transitions between compartments are linear, any changes in the Susceptible population are a result of individuals transferring to the Infected population. A requirement is that the starting Susceptible population must be ≥ 0 since there can not be a negative population size.

$$\frac{dI}{dt} = \frac{\beta IS}{N} - \gamma I, \qquad I(0) = I_0 \geq 0$$

The change in infected individuals is the number of newly transferred individuals from the Susceptible compartment minus any individuals who have already recovered. As defined earlier, γI is equivalent to the number of infected individuals past a certain time period, who can be called "recovered" or "removed".

$$\frac{dR}{dt} = \gamma I, \qquad R(0) = R_0 \geq 0$$

The change in recovered individuals is simply the number of infected individuals who cross the average infectious period and thus are either dead or recovered.

Beyond the basic SIR model detailed in Kermack-McKendrick's theory, there exists a wide range of models specifically for different cases. For instance, in the SIR model, deceased individuals are treated the same as recovered but in the SIRD model they are seperated into another compartment. Furthermore some diseases such as measles can lead to maternally-derived immunity when babies are born and achieve immunity

due to antibodies passed through the placenta. This gives rise to the MSIR model where M stands for "maternally derived immunity" and SIR is the same as before.

Another compartmental model that is relatively common is the SEIR model where E stands for Exposed individuals. The difference between the SEIR model and the simple SIR model is that diseases may have an incubation period where individuals have been infected but cannot transmit the disease yet. Thus, these individuals are placed in the Exposed compartment.

2.3 Agent-Based Models

Agent-based models, also known as ABMs, are a relatively recent type of simulation models which allow for computational approaches in simulating infectious diseases. One of the first ABMs was published in 1996 by Joshua Epstein and Robert Axtell [20]. The model consists of a population of agents, each with their own pre-determined characteristics, that undergo a simulation of interactions in an environment according to a set of rules [47]. ABMs do not have a strict definition of agents as agents can portray any kind of populations such as individuals or households. An agent's characteristics can include features such as health status or demographics for an individual agent. Although there are certain rules dictating the actions that agents can take, ABMs are non-deterministic (stochastic) as innate randomness in the model allows for varied population changes. In the case of epidemiology, agents can be inserted into a social network where rules dictate agent interactions in the network and their reactions to infectious diseases [19].

In comparison to compartmental models, ABMs allow for a greater range of individualized factors and more complex interactions which in turn produces more observations into reactions from individual agents and the population as a whole. For

instance some compartmental models such as Kermack-McKendrick's SIR model assume a well-mixed population where individuals have equal chances of contacting infected individuals and thus cannot account for the complex social interactions inherent in a pandemic situation. Although there have been efforts to create compartmental models that can take into account varying levels of social mixing, they cannot represent contacts between distinct individuals [45].

Because of their effectiveness in modelling infectious diseases and reactions to interventions, ABMs have been used by a large range of institutions such as the CDC and John Hopkins Medical School for prior infectious diseases [39].

2.4 Contact Networks

As mentioned in previous sections, modelling the contacts between distinct individuals is a difficult task that is very important for realistic representations of human populations. A contact network aims to make this task easier by containing information about contacts between individuals such as location, frequency, and duration of contacts [12]. Furthermore, contact networks can contain important information about communities such as relevant social circles for individuals. Thanks to technological advances, observations can be made in a real-life environment by using GPS and Bluetooth. Contact networks are not necessarily only used for epidemiological studies as they are useful for studying and modelling human social networks. An example of a contact network is the Copenhagen Network which was collected by researchers studying approximately 700 university students over one academic year [42]. The researchers used Bluetooth to identify physical proximity, phone call, text message, and Facebook networks to identify communication networks. An example of

the Copenhagen's Bluetooth contact network over a span of 40 minutes can be seen in Figure 2.2.

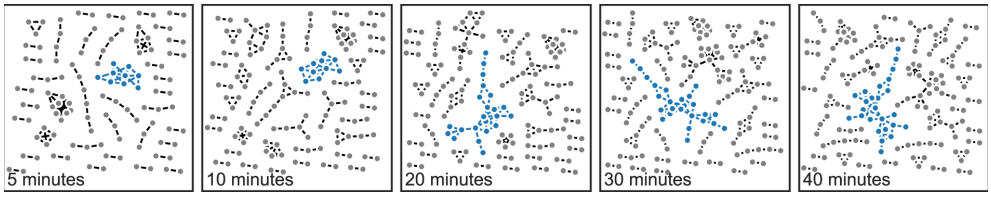

Figure 2.2: A visualization of Bluetooth networksin the Copenhagen Network over time [42]

As seen in the Copenhagen Network, not all data is relevant to modelling the spread of an infectious disease; however, data about physical contact and its duration is especially helpful in identifying meaningful contact and its frequency among individuals.

2.5 Epidemic Parameters

Part of the goal of these disease models is to provide a prediction of how an epidemic spread will occur. In order to measure the spread of an epidemic and the effects of the epidemic spread, there exist several calculated epidemic parameters. As researchers use epidemic models to model different interventions, these parameters are important for predicting the effects of such interventions.

2.5.1 R_0, The Basic Reproduction Number

R_0 is commonly known as the basic reproductive number and refers to the average number of infections that an infected individual will cause. It is commonly used to analyze how contagious an infectious disease is. For example a $R_0 = 3$ means that the average individual will infect 3 other non-infected individuals. R_0 is a non-negative real number that has two important delineations for possible values:

- **Case 1 ($R_0 < 1$) :** If R_0 is less than one then that means, on average, an infected individual will infect less than one other person and the infectious disease will eventually die out as the infected population is unable to sustain itself.

- **Case 2 ($R_0 \geq 1$) :** If R_0 is greater than or equal to one, this means that on average an infected individual will infect at least one other individual and the disease will be able to sustain itself and stay stable or become widespread.

The R_0 is influenced by 3 factors: the disease's infectious period, the average contact rate, and the mode of transmission. This is due to the fact that the longer a disease is infectious, the more likely an infected individual will infect other individuals. The higher the average contact rate, the more chances that an infected individual can infect others. The mode of transmission is especially important since diseases that are air-transmitted are easily transmitted compared to diseases such as HIV which are transmitted via bodily fluids. Thus, the R_0 could be represented as such:

$$R_0 = \tau \cdot \bar{c} \cdot d$$

Where τ is the probability of infection between a susceptible individual and an infected individual (given contact), $\bar{c}$ is the average contract rate for infected individuals, and d is the disease's infectious period [28].

Chapter 3

RELATED WORKS

3.1 Prior Pandemic Studies

The study of how pandemics spread and intervention methods to curtail a vast spread has been studied by many researchers in the past.

In 2008, Davey and Glass published a paper about community mitigation strategies for the Influenza Pandemic [16]. The authors used a networked agent-based computational model, Loki-Infect, and child sequestering & all-community sequestering methods. Child sequestering is the strategy of keeping children and teenagers 18 years and younger at home. All-community sequestering is similar except with all community members. Similar to the compartments in a compartmental model, individuals could be given one of seven classifications (uninfected, latently infected, infected presymptomatic, infected symptomatic, infected asymptomatic, immune, or dead). The Loki-Infect model selects transmission opportunities stochastically and can be tuned based on hyperparameters such as infectivity of the virus, susceptibility of individual, and infectiousness of transmitting persons. They found that child sequestering by itself did not control the epidemic enough and required community sequestering to meet the goal of reducing infection rates. Upon reaching a threshold for reduced infection rates, they found that triggering restrictions again upon reaching 10-cases was very effective in flattening the infection rate. One key note they noticed was that compliance to epidemic strategies was vitally important, otherwise having stricter thresholds could still lead to the opposite effect where a majority of the population became infected.

In 2009, when the H5N1 avian flu pandemic started, Araz et al. studied the spread of the pandemic throughout Arizona and studied the simulation of school closures and how it affected the pandemic [4]. Authors used a compartmental model (SEIR) and assumed only exposed individuals were travelling. The researchers looked at the period that schools would be closed for and found that if only closed for 8 weeks (with limitations for gatherings), the student infection rate due to a second wave would be 20.5% and the death rate 0.59%. On the other extreme, if the schools were closed for 9 months, the infection rate would be 3.35% and the death rate 0.1%. Furthermore, they found that closing schools earlier would not affect the total rate of population infection (within a span of 3 weeks) but would increase student deaths.

In 2014, Gemmetto, Barrat, and Cattuto published a paper focused on analyzing the mitigation of infectious diseases at schools [22]. They modelled different mitigation measures involving the closure of school classes, grades, or even the entire school. The authors used a contact network based off of data collected from a primary school in Lyon, France. The authors found that closing individual classes for 5 to 6 days resulted in the same epidemic curve which indicated that classes should be closed for about a school week for the maximum effect. On the other hand, closing a school grade vs. closing the whole school results in the same amount of infections but a slower reduction in infection rate for grade closures.

Granell and Mucha published a 2018 paper which presented a meta-population based model to describe disease transmission where individuals' mobility patterns were clearly defined [23]. Meta-population models are temporal and spatial models that study interactions amongst different populations of the same species. Different from some other meta-population based models which assumed completely well mixed or completely structured populations, the authors' model presumed a recurrent mobility pattern between an individual's home and common destinations with mixing. They

found that the spread of an epidemic was dependent on the mobility of individuals and thus when mobility of infected individuals were gradually restricted, the epidemic came closer to becoming extinct.

3.2 Covid-19 Studies

Due to the large impact that COVID-19 had on the world at large, there have been a slew of papers focused on modelling COVID-19 and analyzing intervention methods.

3.2.1 Agent Based Models (ABM)

Kucharski et al. explored the effectiveness of isolation scenarios in terms of newly infected and newly quarantined populations [32]. Using the BBC pandemic dataset of around 40 thousand UK participants the researchers constructed a contact network model. The BBC pandemic dataset was created by Klepac, et al for the BBC documentary "Contagion! The BBC Four Pandemic" [31]. The dataset focused on self-reported social mixing contact data and allowed for fine-scale age-specific contact matrices. Kucharski et al.'s modelling found that testing and contact tracing strategies reduced reproduction more than mass testing or self isolation by themselves. Furthermore, when looking at restrictions for the size of events, they found that the event sizes had to be very small (less than 10-20) before a reduction in reproduction would occur.

Rockett et al. used an agent-based model based off of the Australian population census and simulated disease transmission in a multi-layered network [41]. The authors simulated several mixing contexts such as households, neighborhoods (cluster of four households), and local government areas. Furthermore, they specified a special

case of wider community transmission where a household member infects a community member who then infects another of the original household's members thereby throwing uncertainty in whether the disease was transmitted in the household or an outside member. By continually testing new cases against cases that previously had no known genomic link, the authors were able to newly identify clusters of infection.

3.2.2 Compartmental Models

Arenas et al. used a Microscopic Markov Chain Approach mobility model (MMCA) to model the spread of COVID-19 and studied control measures and estimated the peak incidence of COVID-19 in Spain [5]. MMCA is a set of discrete-time equations for the probability of individual nodes in a network to be infected which allows the construction of a phase diagram of the different infection models and their critical properties. Their model takes into account asymptomatic individuals and ICU patients by creating a model with 7 compartments composing the meta-population along with a split between the younger, middle-aged, and elderly sub-population. Besides the common SEIR compartments, the authors added an Asymptomatic Infections, ICU Hospitalized, and Dead compartment. The model also takes into account the relatively more silent transmission among the younger population, the spatial dissemination by mobile adults, and severe symptoms caused in elderly that affect the medical resources available to treat patients. The population is distributed into a set of patches which as a baseline, allow inter-patch movement with no restrictions. Using epidemiological parameters from the COVID-19 outbreak in Spain they found that lower isolation rates led to the epidemic curve flattening which led to longer epidemic periods with less impact on society. Larger isolation rates led to a reduced epidemic size and a shorter epidemic wave duration.

The practice of full population masking is widely adopted in Eastern countries; however, it is less common in their Western counterparts. Eikenberry et al. aimed to model the effectiveness of masks (including homemade cloth masks) on a massive scale during COVID-19 [18]. The authors used a Kermack-McKendrick-type compartmental mathematical model instead of an agent-based model. Using a previously developed SEIR model for transmission dynamics, they developed a two-group model which separated the population based on whether they used face masks. The authors found that having more mask coverage along with effective masks is important for protecting the population. Furthermore, they noted that delaying mask adoption among the population could undermine the efficacy of mass mask usage. In their conclusion they urged that masks should be adopted early on regardless of transmission intensities.

Chung and Chew used a SEIR model along with an additional multiplex and temporal network to model the spread of COVID-19 in Singapore [13]. The multiplex network is a network composed of multiple overlapping networks which each describe various social connections. The aim of their multiplex network is to emulate real-world social interactions and more effectively identify exit and prevention strategies for COVID-19. Their multiplex network consisted of a household, dormitory, workplace, temporal crowd, and temporal social gathering network. The household network is densely connected and the population distribution is assumed to be a Poisson distribution. The dormitory network in comparison with the household network is much more connected and has a higher number of residents. The workplace network models interactions within and between workplaces and the population is assumed to be Gamma distributed. The school network is modeled similar to the workplace network. Random groups of agents make up a "social interaction" group and are used to fully connect the temporal network. 45% of the household network are connected to the workplace network (students are represented as "working" at school) and 90% of

dormitory workers are included in the workplace network. Using a branching process estimator to evaluate the reproduction number (R0), they found that the gradual lifting of social restrictions would flatten the epidemic curve while an immediate return to social norm would lead to another huge wave.

Small and Cavanagh went an alternate route compared to many other COVID-19 compartmental modelling papers where instead of using precise knowledge of the epidemic's transmission parameters, they demonstrated that a detailed enough contact network is sufficient for capturing the spread of COVID-19 [46]. Similar to other compartmental models they use SEIR which stand for Susceptible, Exposed, Infected, and Removed. The model proposed is a network switching model where the topology of the network changes reflect different mitigation and control strategies. Instead of a full-mixing approach the authors proposed an adjacency matrix of the contact network where susceptible nodes can become exposed if there is an infected node nearby and the exposed nodes would become infected with a certain probability. Similarly, an infected node becomes removed at a certain probability. Then using their compartmental model they modeled four different kinds of control strategies:

1. No-control strategy: The network is modelled as a scale-free network. A scale-free network is when the probability of nodes having a certain amount of connections follows the power law. In this case this means that the majority of individuals have a smaller number of connections but a small minority are able to have an arbitrarily large number of contacts. This small minority allows for any number of secondary transmissions and thus guarantees continued transmission. This assumption of scale-free networks is acceptable since researchers have found that the spread of Covid-19 follows the power law [48]

2. Hard-isolation strategy: Using a two dimensional lattice, each node has four adjacent neighbors. The nodes in this strategy do not move geographically and can maybe correspond to familial units.

3. No mass gatherings strategy: Using a random graph with a degree of 4, nodes make random connections that avoid multi-edges and self-loops. The graph is binomial and thus there is a constant fixed probability that two random nodes are linked which leads to an exponential spread but no super-spreader events (where one individual infects a large amount).

4. Social distancing strategy: The authors used a small-world lattice where the network is constructed as a regular lattice but each edge has a probability of being disconnected and rewired to another random node. Small-world networks are when most nodes in the network are not neighbors but are still reachable by any other node via. a series of hops. As such, nodes in the small-world lattice are geographically constrained but some fraction of the nodes have long range connections.

The parameters of their model were as follows:

- Population Size
- Threshold infection load for first infection
- Probability of transferring from Susceptible to Exposed
- Probability of transferring from Exposed to Infected
- Probability of transferring from Infected to Removed

Testing their model on Perth, Western Australia with a population of approximately 2.1 million, an infection threshold of 150, exposed probability of 0.2 and $\frac{1}{12}$, infection

probability of $\frac{1}{7}$, and recovery probability of $\frac{1}{14}$ and $\frac{1}{4}$ (different probabilities are for pre-peak and post-peak, respectively). The authors found that their model's results had a similar rate of spread compared with the transmission data for Australia.

Chapter 4

COVID-19 MODEL

4.1 Cambria Case Study Description

As one of the methods to test our model, we decided to start with the small local community, Cambria village in San Luis Obispo County, California, United States. Using the US Census Bureau data for July 1, 2019, Cambria's population is 5,647 [7]. The model for this Case Study will be a simple SIR model where Susceptible individuals can become infected upon contact with Infected individuals. After approximately 14 days, an individual is assumed to be Recovered.

4.1.1 Case Study Assumptions

As part of the assumptions for Cambria, the first is that a majority of the population are elderly as the US Census reveals that 41% of the population is 65 years old and over. As part of this population assumption, the distribution of household sizes no longer follows the Poisson Distribution mentioned in Section 4.2.5 but is instead a custom distribution of 20% 1-person, 50% 2-person, and 30% 3-person homes to account for more elderly individuals living with caretakers or other adults.

The second assumptions is about the travelling patterns of individuals in this community. In order to simplify assumptions, one individual from each household is assumed to be the individual traveling to community centers and only that individual will travel. All other individuals are assumed to be stuck in the household unable to travel. Understandably this does add an additional layer of inaccuracy to our

ABM as in real life, all adult individuals can travel to community centers. We believe this realistically approximates the behavior of the community during lockdown. We imagine that the community centers in Cambria are grocery stores since there are only two major ones.

The third assumption is that infected individuals will become recovered after 13-15 days, which does not take into account deaths, hospitalizations, and longer tail infection periods.

The fourth assumption is that there are no external contacts from outside of Cambria's community thus all infections come from inside the community including the initial infection.

4.2 Model Design

In designing the model to simulate COVID-19's spread we decided to use the Agent-Based Model (ABM) approach in part due to the effectiveness of ABMs in modelling individual interactions and simulating population dynamics.

4.2.1 Agent Design

Each of the agents in our model represent an individual inside of a community's population. All agents belong to a household which may have 0-3 other individuals also belonging to that household. An agent will always belong to the same household.

4.2.2 Environment Design

The model's environment is divided into discrete time-steps to provide a frame of reference for the epidemic spread and results. In order to better simulate a real day's 24 hour period, the model delineates four discrete time-steps to make up one day. The time-steps that make up a day are Morning, Afternoon, Evening, and Late Evening. During the Morning, Afternoon, and Evening time-steps, agents are allowed to "travel" to a community center as long as their travel is consistent with the experiment's parameters. At the Late Evening time-step, all agents are to return home no matter their location. A community center is chosen to simulate essential areas that individuals have to travel to, such as grocery stores and workplaces. The idea of a community center as a focal point for individual travel is similar to related papers that used them to better model individual mobility [23] [13].

As part of the environment design and experimental parameters, individuals may travel to a community center at certain days of a week or households determine a single individual that can travel while the other individuals in the household stay at home. This seems to be a reasonable assumption for an aged population's mobility in a lockdown scenario.

4.2.3 Network Design

Our model is a directed graph $G = (V, E)$ where each node $v \in V$ represents an individual agent and each edge $e \in E$ denotes nodes that are in extensive contact. Extensive contact is defined as enough contact that the transmission of disease is possible. Each node v belongs to a clique C that represents the individual's household. A clique is defined as a graph where each node is connected with every other node. As befitting a clique, each individual in a household has directed edges to and from

every other individual in the household. When a node "travels", all edges they are currently connected to are cut and the node forms new edges to other nodes at their destination. The number of edges formed is dependent on the destination. This process is the same whether nodes are traveling to a community center or back to their household. Although later on the direction of the edges in the graph were not ultimately expanded upon and can be treated as bidirectional edges, the directed edges were kept for future flexibility.

An example of node movement over 4 timesteps is in Figure 4.1. There you can see that at timestep 1, all the nodes are in their own household. At timestep 2, nodes 1, 5, 8, and 14 move from their respective household to a community center which is shown by edges connecting the nodes together. At timestep 3 the previous nodes return back to their own household and we can see that nodes 0 and 10 also connect together by meeting at a community center. At timestep 4, all the nodes return back to their own household since this is our "Late Evening" timestep.

4.2.4 Implementation

Our ABM is built from the Python language using libraries such as numpy and networkx to handle the network implementation and mathematical computing. The rest of the ABM is built from scratch and uses a state-based design pattern to handle a majority of the logic for travelling agents and agent information upkeep. On average for a population of 5.6k, the program takes 0.1-0.2 seconds to run a single timestep. This translates to 0.4-0.8 seconds for a single day. The program can be run by using flags to enter parameters such as length of the experiment, infectious rate, exit factors, and others.

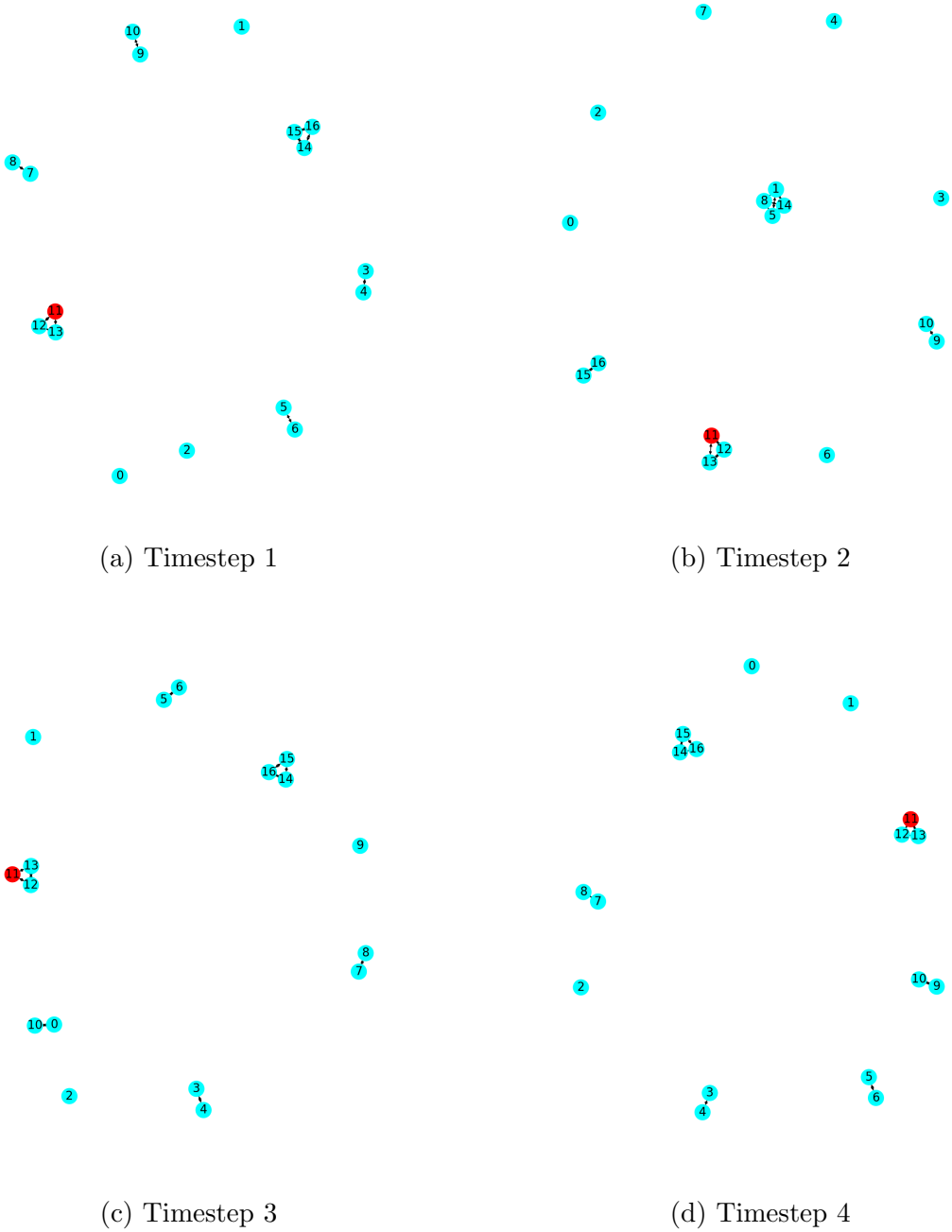

(a) Timestep 1

(b) Timestep 2

(c) Timestep 3

(d) Timestep 4

Figure 4.1: Sample of node movement in graph over 4 timesteps

In order to run the experiments, we created a bash script that would run the program on a variable amount of cores as a method of simulating parallel computing for our program. Upon running our experiments and outputting the data to a text file, we used python scripts to either read the data and produce data reports or produce graphs used in this thesis.

4.2.5 Epidemic Model Assumptions

There are several assumptions that we are making for the epidemic's parameters and design. The first is that the infection probability upon contact between an infected individual and an exposed individual is approximately 16%. This percentage was chosen by rounding the overall household secondary attack rate found by a meta-analysis of 54 studies [35]. Although the percentage provided by the paper is specifically for household secondary attack rates which has more extended contact between individuals when compared to community centers like grocery stores, we will assume the worst case in terms of contact and use this infection probability for community centers also.

A paper by Cevik and Marcus et al. using data from Cevik and Tate et al. found that the viral load for Covid-19 had an incubation period of approximately 6 days and that the infectious period starts 2 days before symptom onset and approximately 10 days after symptom onset [10] [11]. An analysis of the viral load showed the following:

- 2 days before symptom onset to the day of symptom onset: A rise from minimal zero load to peak viral load
- The day of symptom onset to 5 days after: Stable and consistent peak viral load levels

- 5 days after symptom onset to 10 days after: Decreasing viral load to minimal levels.

This is visualized in the Cevik and Marcus et al. paper and is seen in Figure 4.2 [10]

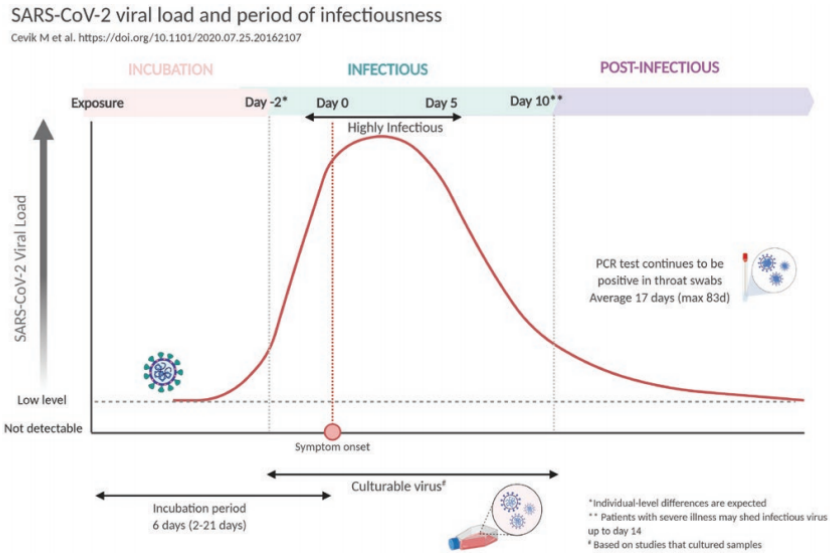

Figure 4.2: Visualization of viral load of Covid-19 over time and in relation to symptom onset [10]

Using this analysis on viral load, we alter the infection probability based on three different periods, 2 days before symptom onset to the day of symptom onset, the day of symptom onset to 5 days afterwards, and 5 days afterwards to 10 days afterwards. This can be seen in Table 4.1. To account for varying periods of incubation and infection period as not all infected individuals are the same, they are allowed to randomly vary their incubation and recovery period by ± 1.

Table 4.1: Time periods in relation to weighted infection probability

Days	Infection Ratio
-2 to 0	0.75
0 to 5	1.0
5 to 10	0.5

Another assumption is the contact rate for individuals in a household and in community centers. It is assumed that the individuals in a household are fully connected

and have equal chances of infection for each other individual. Household sizes are assumed to be distributed according to a Poisson distribution with modifications for specific cases [27]. Specific cases can include a larger emphasis on 2-3 family homes for a community with a mostly older population as most elderly typically live with a caretaker or family.

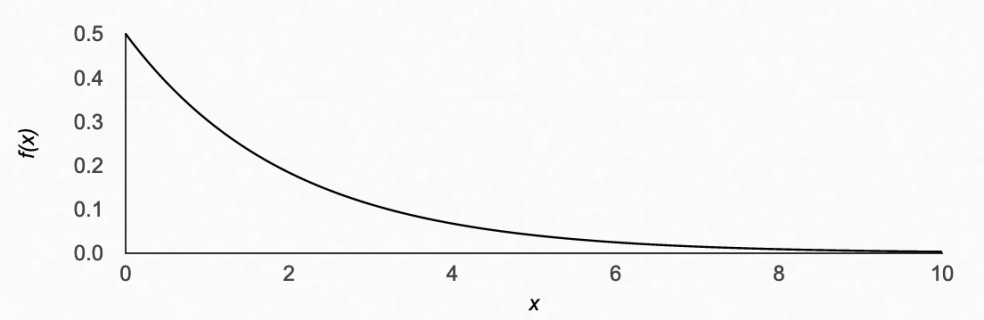

Figure 4.3: Sample distribution for a Community Center of size 30

As community centers are not typically fully connected, we assumed that individuals will be interacting with a small subgroup in the community center. We chose a gamma distribution with custom parameters to ensure that an individual mostly comes into contact with a small amount of individuals such that the average contact rate for infected to susceptible populations is relatively low. The max range of the distribution is a third of the community center's population while the minimum is one contact. The max range is set arbitrarily and can be changed to fit different scenarios. This gamma distribution is skewed right and an example can be seen in Figure 4.3 for a community center of size 30.

In the example, there is a 50% chance of zero contacts (which is rounded to one since our minimum is one) and a 1.11% chance of 9 or more contacts.

Chapter 5

RESULTS

5.1 Experiment Result Metrics

For analyzing the results of our experiments, we will mainly look at the infected population and metrics surrounding them. Two main metrics for an infectious population are the total number of individuals infected over the course of the experiment and the amount of individuals infected during the peak of the epidemic. The first metric is used to identify the total spread of the disease and the second metric can be used to visualize the severity of the disease during its peak which is important for modelling the load of ICUs. Having a large infectious peak does not necessarily denote that the disease is the most infectious but it does raise some flags and promotes a deeper study of the experiment.

The third metric that we use is the R_0 of the disease. As defined in Section 2.5.1, the R_0 is commonly used to measure the average amount of infections that an infected individual will cause. This helps us identify how contagious an infectious disease is. We will use the same calculation from our definition where given τ is the probability of infection, $\bar{c}$ the average contact rate for infected individuals, and d is the diseases' infectious period, $R_0 = \tau * \bar{c} * d$.

Using these 3 main metrics we hope to understand the general progression of the disease in each experiment and when needed, to dive deeper into the intricacies of the experiment's events.

5.2 Cambria Case Study Experiments and Results

The experiments we will run for the Cambria case study will include the following:

1. Covid-19 spread without any interventions
2. Covid-19 spread with Mobility Restrictions (for all individuals)
3. Covid-19 spread with Mobility Restrictions and Mask Usage
4. Covid-19 spread with Quarantining

5.2.1 No Interventions

In order to simulate the "no intervention" scenario, individuals will exit freely between 5 to 7 times a week and upon symptoms appearing will still travel around with no interventions by individual or isolation strategies. Each of the no intervention scenarios allows for a variable infection probability. This is because the infection probability we are using may have a bias based on the location and different behaviors during data collection. Thus by simulating different infection probabilities we can achieve a deeper understanding of interventions' affects on people. In order to simulate the freely exiting factor of individuals, we use an Exit Factor which tries to evenly space out the days an individual leaves. For example, given an Exit Factor of 3, an individual's first departing day is chosen randomly but the next day is 2 days away and the following day is also 2 days away. So for a randomly chosen day of Monday, the next exiting day is Wednesday, and the following is Friday.

Each simulation was run for 100 days and 10 times each to ensure consistency. One of the first data points we are interested in is the amount of infected individuals during the peak of Covid-19's spread as an indication of how far the disease was able

to spread. This can be seen in Table 5.1 where for each Exit Factor and different Infectious Probabilities, the average percentage of infected individuals across 10 runs is listed. That is to say a simulation where individuals travel 5 times a week and where the disease has a 16% chance of infecting individuals during contact was able to infect 91.9% of the population during its peak. We believe this to be an underestimate as people do not generally travel so regularly.

Table 5.1: Average Peak Infected Population for given Exit Factor and Infection Probability

		Infection Probability				
		0.16	**.2**	**.3**	**.4**	**.5**
Exit Factor	**5**	0.918	0.942	0.970	0.983	0.989
	6	0.942	0.961	0.985	0.992	0.996
	7	0.955	0.973	0.990	0.996	0.998

When plotting the results of the ten simulations, we find that the results match in terms of general trend for infected populations while differing only in when the infectious spike occurs. The changes in Infectious Probability are straightforward in increasing the size of the infected population as seen in Table 5.1. As for the SIR dynamics over the course of this experiment, an example of this can be found in Figure 5.2. The figure depicts the SIR dynamics for an Exit Factor of 5 (exiting 5 times a week) and an Infectious Probability of 0.2 (20%). The x axis consists of the experiment's 100 day time while the y axis is the population percentage. Each of the 10 runs for a given Exit Factor and Infectious Probability are shown in the figure to demonstrate the experiment's consistency.

To visualize the average runs for two realistic Infectious Probabilities (16% and 30%) we plotted the average infectious population for each Exit Factor in Figure 5.1. There we can see that as expected, the population with an Exit Factor of 7 and Infectious Probability of 30% had the largest spike on average. Furthermore we can also see that the experiments with an Infectious Probability of 16% have an infection spike later

than the corresponding experiments with an Infectious Probability of 30%. Another result that follows from expectations is that the lower Infectious Probabilities resulted in lower infection spikes.

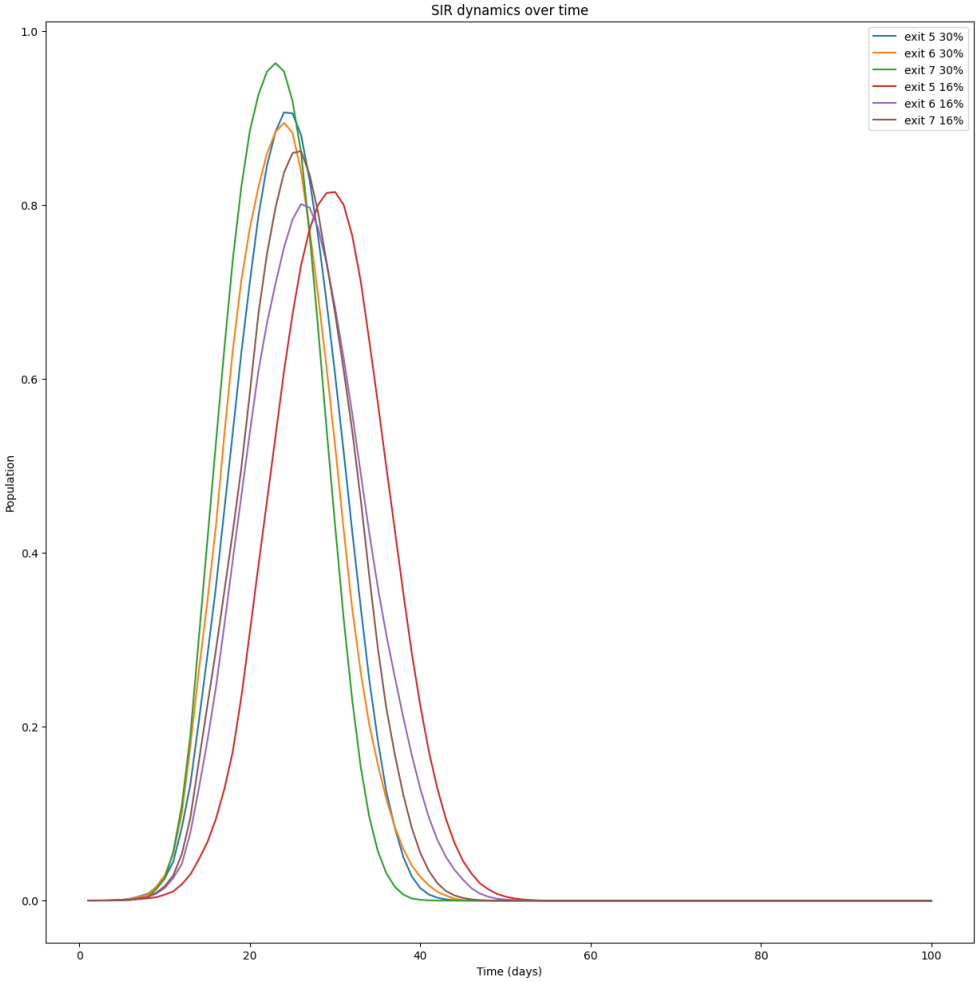

Figure 5.1: Infectious Dynamics of Exit Factor 5-7 and Infectious Probability 0.16 and 0.3

As for the results of the Exit Factor, we can see that higher Exit Factors result in a higher proportion of the population infected. Looking at the SIR dynamics over the 100 day period we find that the infected population achieves a steep spike in infections within 40 days of the introduction of an infected individual into the community. Immediately before and after the infected population spike, we can see a steep decrease in the susceptible population as individuals are rapidly infected. When

compared with a simulation with an Exit Factor of 6 and the same infectious period (Appendix A.1) we can find that the infection spike is slightly higher, the infection spike occurs earlier but otherwise it results in a similar behavior. The infection lasts approximately 40-60 days even for the experiment with the lowest infection chance (Exit factor of 5 and Infectious Probability of 0.16). By the end of the infection, the virus dies out since there are no more readily available Susceptible individuals to continue the virus' spread.

As seen in the Figure 5.2, the infected population is roughly 99-100% of the entire population thus completely infecting the community.

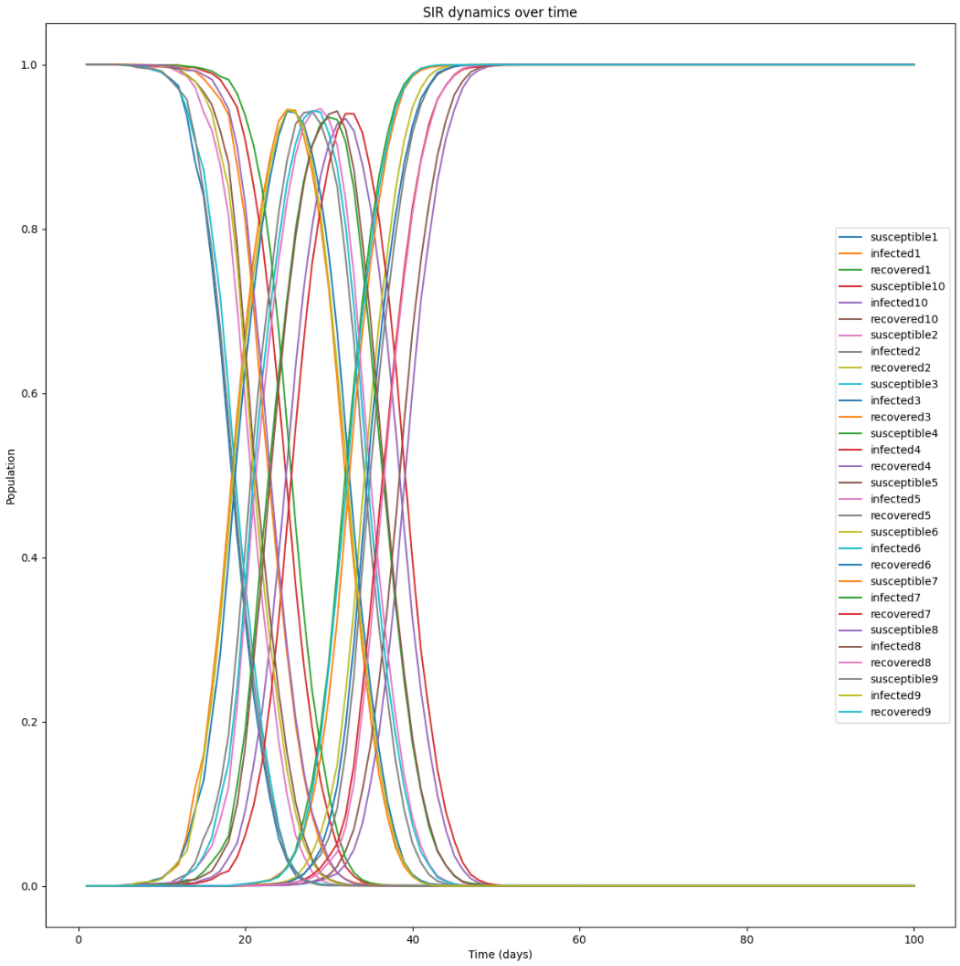

Figure 5.2: SIR Dynamics of Exit Factor 5 and Infectious Probability 0.2

As a base case for modelling the spread of Covid-19, these results serve as an inspection of how the model occurs given zero interventions and encouraging the spread of the disease. As evidenced by the exponential growth of the infectious population, the disease performs as expected.

5.2.2 Mobility Restrictions for all individuals

Mobility restrictions for all individuals is characterized by limiting how often an individual exits during a week. As the no restriction experiment consisted of individuals leaving 5 to 7 days a week, this experiment consists of individuals leaving 1 to 4 days a week. Similar to the prior experiment, each respective Exit Factor and Infectious Probability were ran for 100 days and 10 times each.

5.2.2.1 Comparison with No Intervention case

Table 5.2: Average Peak Infected Population for a Mobility Restricted community

		Infection Probability				
		0.16	**0.2**	**0.3**	**0.4**	**0.5**
Exit Factor	**1**	0.001	0.004	0.003	0.014	0.016
	2	0.148	0.166	0.174	0.233	0.241
	3	0.436	0.458	0.476	0.494	0.515
	4	0.492	0.462	0.481	0.456	0.522
	5	0.918	0.942	0.970	0.983	0.989

The results for the infected population's peak can be seen in Table 5.2. The table also includes the Exit Factor of 5 as a benchmark from the no intervention case. In comparison to the benchmark we can see that average peak infected population for each given Exit Factor and each Infectious Probability is relatively low. Furthermore we can see that there is a tipping point between an Exit Factor of 4 or 5 no matter the Infectious Probability as the Infectious Probability jumps a significant amount.

For instance, at an Exit Factor of 4 and Infectious Probability of 0.5, we can see that the highest percentage of population that was infected at one time was 54.7% while in comparison to an Exit Factor of 5 and the same Infectious Probability (0.5) we see that the highest percentage infected was 98.9%.

5.2.2.2 Decrease in peak even with increased Infectivity

We can see an observed decrease of peak infected individuals even though the Infectious Probability is increasing. For an Exit Factor of 1, the peak decreases from Infectious Probability of 0.2 to 0.3. For an Exit Factor of 4, the peak decreases from infection probability 0.16 to 0.2 and 0.3 to 0.4. A concise summary of these decreases is in Table 5.3. Exit factors 2 and 3 are not in the table because their peaks were monotonically increasing and dashes are to signify that the value was lower than the next peak.

Table 5.3: Observed decrease in peak of infected individuals

		Infection Probability			
		0.16	**0.2**	**0.3**	**0.4**
Exit Factor	**1**	-	0.004	0.003	-
	4	0.492	0.462	0.481	0.456

Looking at the raw data for each simulation we found that these could be explained by an inopportune placement of the initial infected individual. Given a low Exit Factor and low Infectious Probability and the assumption that individuals' infectious periods are approximately a 12 day period (from Section 4.2.5), an individual may only exit once or twice during this entire 12 day period and if they exit while their viral load is relatively low they may not be able to infect as many individuals as they should.

However this may not be as feasible of an explanation for the case of Exit Factor 4. Individuals can exit about 3 times during the infectious period.

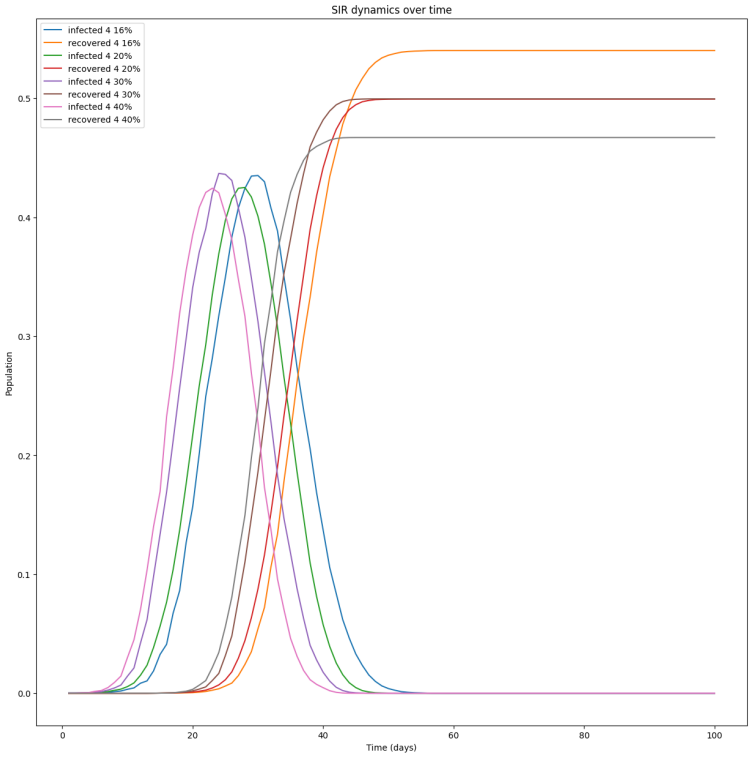

Figure 5.3: IR Dynamics for an Exit Factor of 4

Looking through the logs we can find that in part due to the higher Infectivity rate of the disease, there was a relatively earlier spike in infections which led to an earlier recovery rate of individuals. The earlier spike of recovered individuals decelerates the spread of infected individuals, as the infection is unable to find enough susceptible individuals to continue increasing exponentially.

This can be seen in Figure 5.3 which graphs the infectious and recovered population for Exit Factor 4 and Infectious Probabilities 16%, 20%, 30%, and 40%. In the figure we see that for each increase in Infectious Probability, the infected peak is earlier. For instance for 40%, the peak is around day 20 but is around day 30 for 16%. Similarly, the recovery curve starts increasing earlier for higher infectious rates.

Table 5.4: Total average infected population percentage

		Infection Probability				
		0.16	**.2**	**.3**	**.4**	**.5**
Exit Factor	**1**	.002	0.008	0.009	0.03	0.031
	2	0.228	0.228	0.205	0.256	0.259
	3	0.531	0.526	0.513	0.518	0.531
	4	0.54	0.499	0.500	0.467	0.527

5.2.2.3 Total percentage of population infected

The total infected population after 100 days averaged over 10 runs can be seen in Table 5.4. We can see a marked increase from an Exit Factor of 2 to an Exit Factor of 3. For an Exit Factor of 2 the total infected population averages between 20% to 26% depending on the infection probability while for an Exit Factor of 3 the total infected population averages between 51% to 53% depending on the infection probability.

An interesting trend is that the total average infected population for an Infectious Probability of 16% vs 20-30% is actually higher in some cases. Looking at the SIR dynamics over time in Figure 5.4, we find that with each increase in Infectious Probability, the spikes in infections happens earlier and earlier.

For instance, for an Exit Factor of 2 and Infectious Probability 16%, the average peak for infections happens around day 42. For an Exit Factor of 2 and Infectious Probability 50%, the average peak for infections happens around day 30. Furthermore, the spikes in infections happens at a greater rate too. Given an Exit Factor of 2, the largest spike in infections is 2.2% of the population when the Infectious Probability is 16%. When the Infectious Probability is 50%, the greatest spike is 4.1%. This is equivalent to a difference in approximately 130 people infected. Thus we can hypothesize that because of the faster spike in infections and mobility restrictions, the infected population recovers at a much faster rate than they can infect other individuals. Although there is an increase in Infectious Probability, the infectious

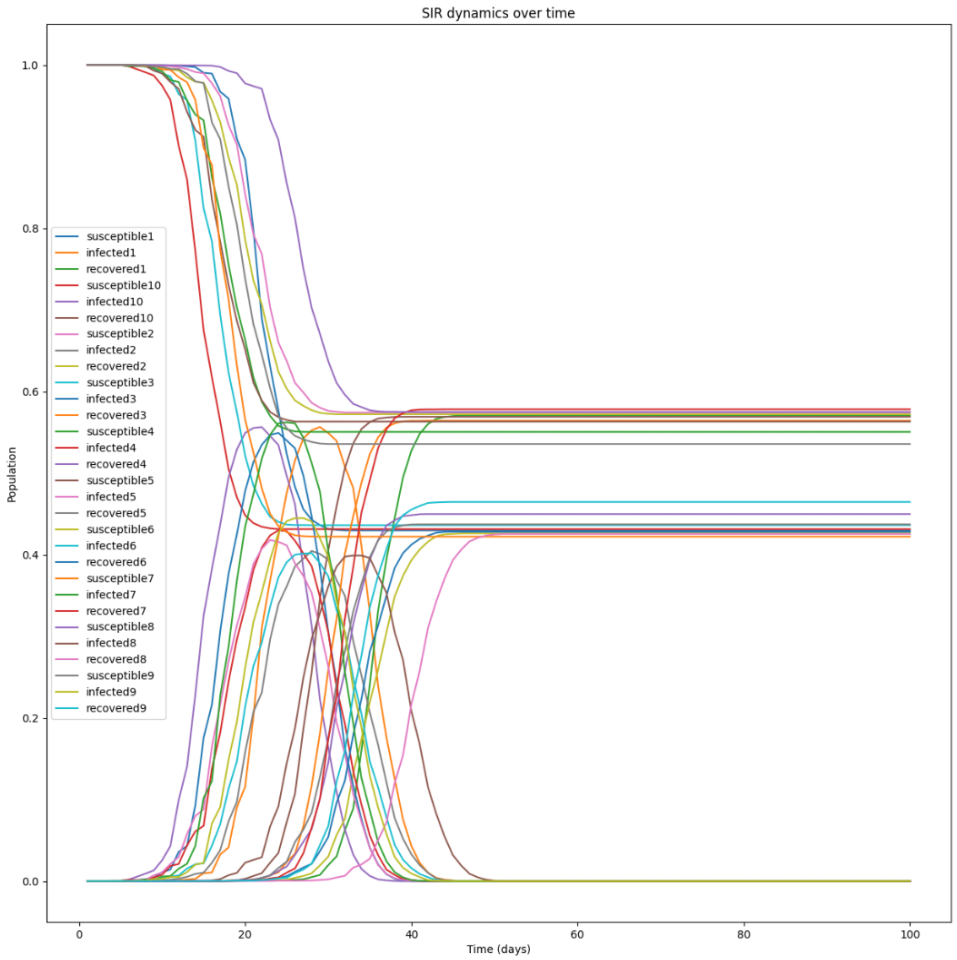

Figure 5.4: SIR Dynamics of Exit Factor 4 and Infectious Probability 0.3

period combined with a reduced number of susceptible individuals results in reduced infections. Thus lower Infectious Probabilities do not necessarily correspond with a lower amount of infected individuals.

5.2.2.4 Measuring R_0

The R_0 for this experiment can be seen in Table **??**. The R_0 follows as expected where lower Exit Factors and lower Infectious Probabilities correlate with a lower R_0 while the opposite also holds true. In comparison to empirically observed R0s for COVID-19, we find that our R_0 values are much lower. A cohort study of transmission

dynamics in California and Washington revealed that the R_0 in Northern California was estimated to be between 1.39 and 1.54 while it was between 2.06 and 2.49 in Southern California [34]. Possible reasons why our R_0 is lower than real-world values is in the model assumptions that we make. One of the bigger assumptions includes

Table 5.5: Average calculated R_0 for a mobility restricted community

	Infection Probability				
Exit Factor	**0.16**	**0.2**	**0.3**	**0.4**	**0.5**
1	0.311	1.037	1.337	2.606	3.564
2	3.055	3.331	3.169	4.612	5.957
3	4.571	5.766	5.592	6.860	9.280
4	5.319	5.125	6.054	7.578	10.589

From the results of this experiment, it shows that mobility restriction may be a promising method of intervention in reducing the amount of infected individuals. Furthermore, this experiment is under the assumption that symptomatic individuals do not change any of their behavior, which is atypical for sick individuals. Even in this worst case, where symptomatic individuals are allowed to travel freely and spread the illness and with a worst case infection probability of 0.5, mobility restrictions are still able to reduce the peak infected population greatly in comparison to Section 5.2.1 where all of the infected populations were 90% and above.

5.2.3 Mobility Restrictions and 100% Mask Usage

This experiment uses the mobility restrictions from Section 5.2.2 in conjunction with simulating mask usage. Mask usage is dictated by a percentage reduction in disease transmission. As part of this experiment, we hope to answer the question of whether mask wearing combined with mobility restrictions are useful in reducing infection rates. As seen in Section 5.2.1, an Exit Factor of 5 is almost similar to Exit Factors of 6 and 7 in terms of the number of infected individuals. Thus, when experimenting with mobility restrictions for this experiment (Exit Factors of 1 to 4) we also included

an Exit Factor of 5 in order to see the results of mask usage on both a non-intervention base case and a mobility restriction case.

5.2.3.1 Assumptions for Mask Wearing

A case-control study of person protective measures (PPE) for Covid-19 in Thailand was published by Doung-ngern et al [17]. In the study, the authors analyzed 839 close contacts of 211 initial infected individuals. The authors found that the adjusted odds ratio for risk of Covid-19 infection and wearing a mask at all times during contact with a Covid-19 patient was 0.23. As such to simulate the usage of masks, we reduced the probability of transmission by a factor of 0.23 when an infected individual wearing a mask is in contact with susceptible individuals. A literature review of studies of the effect of mask wearing on Covid-19 found a similar infection reduction of around 0.7 to 0.79 [6].

As part of the first run for this experiment, it is assumed that everyone is wearing masks although this is not completely accurate when looking at the trends of mask wearing during the Covid-19 pandemic. A paper by Haischer et al. studied the percentage of mask wearers entering retail stores between June and August of 2020. They found that before any store mandates, 80% of individuals were wearing masks and even with state mandates 96% of individuals wore masks [24]. The lowest percentage of mask wearers was before any mandates were announced and was recorded at 41% of individuals.

5.2.3.2 Results

After restricting mobility such that individuals only leave their households a certain amount of times a week and having everyone use masks, the average peak infected population has a small decrease in comparison with just using mobility restrictions.

Table 5.6: Average Peak Infected Population for a mobility restricted and mask wearing community

		Infection Probability				
		0.16	**.2**	**.3**	**.4**	**.5**
Exit Factor	**1**	0.0	0.0	0.0	0.0	0.001
	2	0.003	0.002	0.036	0.088	0.087
	3	0.039	0.133	0.302	0.353	0.419
	4	0.239	0.263	0.361	0.39	0.498
	5	0.619	0.806	0.863	0.909	0.934

For instance, for an Exit Factor of 4 and an infection probability of 50%, which should lead to the most amount of individuals infected, the average peak was 49.8% of the population while with only mobility restrictions it was 51.5%. While this difference is not the largest, other drops in peak infected individuals are noticeable such as for an Exit Factor of 2 and infection probability of 16% which dropped 14.5% from 14.8% to 0.3%. Furthermore, looking at our "no restriction" case, where individuals can leave up to 5 times a week, we found that there is a great decrease for the lower infection probabilities, especially for an infection probability of 16%. Table 5.1 shows that the average peak for a "no intervention" scenario is 91.8% whereas in this case it is 61.9%. This confirms that if 100% of the population wore masks and had mobility restrictions for how often they left, there would be a decrease in infections.

As seen in Section 5.2.2, a lower Infectious Probability does not necessarily correlate with a lower total infected population. This can once again be seen in Table 5.7 where there are several drops in total infected population even with an increase in Infectivity.

Table 5.7: Average Total Infected Population for a mobility restricted and mask wearing community

		Infection Probability				
		0.16	**.2**	**.3**	**.4**	**.5**
Exit Factor	**1**	0.001	0.0	0.001	0.001	0.001
	2	0.008	0.005	0.1	0.198	0.158
	3	0.099	0.284	0.472	0.502	0.526
	4	0.406	0.416	0.478	0.458	0.544
	5	0.89	0.998	1.0	1.0	1.0

For instance, the case when the Exit Factor is 2 and the Infectious Probability is 40% vs. 50%.

Visualizing the infectious population for relatively reasonable Infectious Probability assumptions in Figure 5.5, we can see a remarkable decrease in the peak of infected individuals. In comparison to Figure 5.1 and Figure 5.3 we can see that the infectious curves are flattening out. Following on from the previous analysis of the peak infected population, we can see that the average total infected population is smaller than when there are only mobility restrictions once again verifying that masks result in a lower rate of infections.

Interestingly we can see that two of the curves are slightly flattening out but also extending past day 100. This is in sharp contrast with previous experiments which usually ended before day 100 either due to a completely infected population or due to a completely non-infected population.

5.2.4 Mobility Restrictions and Variable Mask Usage (90% and 80%)

For these experiments, we will vary the percentage of mask wearers along with the mobility restrictions and Infectious Probabilities.

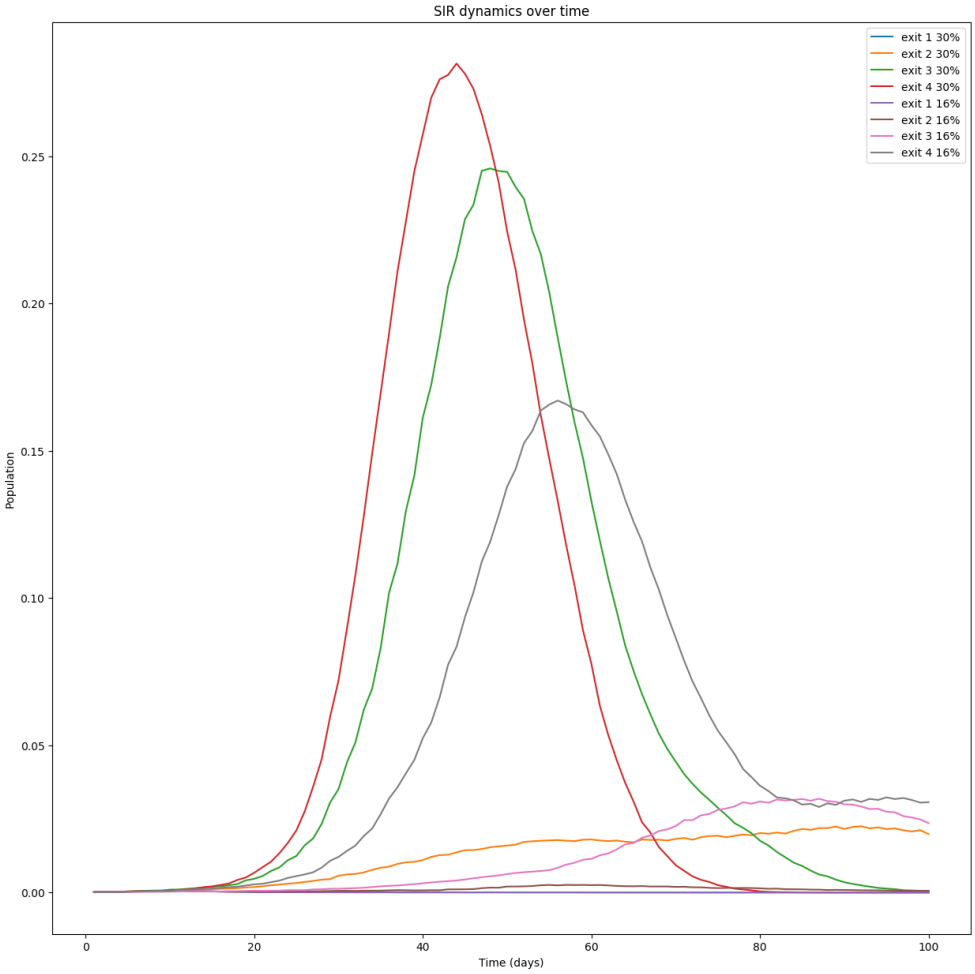

Figure 5.5: Infected population for Infectious Probability 16% and 30%

5.2.4.1 Results

The average total infected population for the 90% and 80% mask usage can be seen in Table 5.8. From there we can see that as expected, there is a higher percentage of the population that gets infected as the percentage of mask wearers decreases. For instance for an Exit Factor of 4 and 20% Infectious Probability, 100% mask usage has 41.6% of the population infected, 90% mask usage has 42.1% of the population infected, and 80% mask usage has 51.1% of the population infected.

Table 5.8: Average total infected population for mobility restrictions combined with 90% and 80% mask usage

	Infection Probability									
	90% Mask Usage					80% Mask Usage				
	.16	**.2**	**.3**	**.4**	**.5**	**.16**	**.2**	**.3**	**.4**	**.5**
1	0.001	0.0	0.001	0.001	0.001	0.001	0.0	0.001	0.0	0.0
2	0.028	0.034	0.113	0.246	0.255	0.041	0.114	0.096	0.253	0.25
3	0.358	0.310	0.464	0.512	0.442	0.402	0.289	0.492	0.411	0.503
4	0.442	0.421	0.471	0.511	0.545	0.423	0.511	0.499	0.545	0.542
5	0.997	0.999	1.0	1.0	1.0	0.998	1.0	1.0	1.0	1.0

Exits

Furthermore, when looking at results from an Infectious probability of 16%, we find that 80% Mask Usage and varying between Exit Factors 3 and 4 results in almost the same infected population. In comparison with just using mobility restrictions, we find that the total infected population decreases for lower Infectious Probabilities (16% to 30%) while remains the same for higher Infectious Probabilities (40 - 50%). In particular, the average range of infected individuals with only mobility restrictions is approximately 50% for Exit Factors 3 & 4. While with 90% Mask Usage, it ranges from 31% to 47% and 29-50% for 80% Mask Usage.

5.2.4.2 Clustered Experiment Results

The increase in infected individuals is not uniform, for instance comparing the total infected for an Exit Factor of 4 and 16% Infectious Probability, we can see that 44.2% of the population is infected with 90% mask usage but only 42.3% of the population is infected with 80% mask usage. Diving deeper into the logs, we can see that for 80% mask usage, each run can be split into 3 different clusters. The first is a total infection of almost 0% (0.0885%), the second is a total infection of about 40-42%, and the third is a total infection of 57-59%. The first cluster is a clear outlier and due to unlucky placement of the initial infection and consists only of 1 out of the 10 runs. The second and third cluster consist of 6 and 3 runs, respectively. 90% mask usage

also falls into similar clusters with the first being roughly 0.0177%, the second being 39%, and the third being 55-57%. The second and third clusters make up 4 and 5 runs respectively. This data can be seen in Table 5.9. After removing the outliers, the average for 90% mask usage is 49.07% and 80% is 47.01%.

Table 5.9: Cluster Analysis of Exit Factor 4

90% Mask Usage	
Cluster	**Number of Runs**
∼0%	1
∼39%	4
∼55-57%	5

80% Mask Usage	
Cluster	**Number of Runs**
∼0%	1
∼40-42%	6
∼57-59%	3

From this we can see that there is a higher occurrence of lower cases in 80% Mask Usage vs 90% Mask Usage. Thus, when calculating the average, we find that the 80% Mask Usage has a lower average total infected population while 90% Mask Usage is higher. However, looking at the clusters we can see that the clusters are higher for 80% Mask Usage (40-42% vs. 39%) and (57-59% vs. 55-57%) which means that with lower mask usage, the population of infected is still higher despite what the average value looks like.

Overall, we still see a decrease in the total infected population when using masks however between 90-80% Mask Usage requires more study on the varying clusters and any additional issues.

5.2.5 100% Quarantine Compliance Strategy

As mentioned in previous experiments, much of our results can be viewed as worst-case scenarios as individuals who are symptomatic do not take steps to prevent further spread of the virus. However, as evidenced by the Covid-19 pandemic, not all individuals can or will stay home if they are symptomatic due to life circumstances or beliefs. Thus, for this section we will explore the impacts of individuals that quar-

antine themselves once symptoms start and the impact of varying the percentage of individuals who will quarantine. Furthermore, we will explore combining this quarantining strategy with prior strategies such as mobility restrictions and mask usage.

To start off, we will assume that 100% individuals will quarantine themselves upon symptoms of Covid-19 showing up. Quarantine consists of individuals staying home and not travelling. Furthermore, we assume that individuals quarantine independently. That is to say a household may have individuals who will or will not quarantine.

Future sections will consist of varying the percentage of the population who will quarantine and making quarantines apply for households even if individuals are not infected.

5.2.5.1 Results

Table 5.10: Average total infected population for 100% Quarantine compliance

		Infection Probability				
		0.16	**0.2**	**0.3**	**0.4**	**0.5**
Exit Factor	**1**	0.001	0.0	0.001	0.0	0.0
	2	0.001	0.009	0.001	0.046	0.076
	3	0.001	0.121	0.238	0.318	0.249
	4	0.13	0.312	0.368	0.31	0.466
	5	0.525	0.749	0.79	0.698	0.5

The first takeaway from our results in Table 5.10 is that 100% Quarantine compliance is effective in reducing the total infected population across the board no matter the Exit Factor and Infectious Probability.

Looking at the results in Table 5.10 we find that almost all of the results are not monotonically increasing as was common in previous sections. In some cases the decrease is not significant, such as Exit Factor 2 and going from 20% to 30% Infec-

tivity which saw a drop of 0.8% being infected. However, other decreases are much more noticeable. For instance, Exit factor of 5 jumped from an average 79% of the total population being infected at a 30% infection chance to an average 50% of the population being infected at 50% infection chance. We have aggregated the drops in infection into Table 5.11. Similar to Table 5.3, the dashes signify that the values are monotonically increasing in order to better visualize the drops. Infectious probability 16% was removed because all the peaks were less than those of Infectious probability 20%. For instance for Exit Factor 2, the dashes for 40% and 50% Infectiousness are 0.046 and 0.076, both of which increase monotonically from 0.001.

Table 5.11: Average total infected population for notable decreases despite infectious increase

		Infection Probability			
		0.2	**0.3**	**0.4**	**0.5**
Exit Factor	**2**	0.009	0.001	-	-
	3	-	-	0.318	0.249
	4	-	0.368	0.31	-
	5	-	0.79	0.698	0.5

5.2.5.2 Clustered Runs

The most concerning result we find is the drop recorded in Exit Factor 5 with a 29% drop in total infected population. Similar to Section 5.2.4 we find that there are very different clusters of results. For instance for an Exit Factor of 5 and Infectivity of 50%, we find that $\frac{4}{10}$ runs resulted in slightly above 0% of the population being infected. On the other hand $\frac{6}{10}$ runs resulted in 99-100% of the population being infected. A hypothesis that can be gleaned from this data is that quarantining allows for more chances to stop the disease before it starts to spread exponentially. Because of the two different extremes, the average total infected population averages out to such a low total infected population. This applies to all of the other notable decreases except

there are 3 clusters in other cases. For instance given an Exit Factor of 3, there are 3 clusters of average infected population, 0-20%, 33-40%, and 53-59%.

In order to better test this hypothesis and because the clustering is so evident, we decided to walk through the experiments step by step.

For the almost 0% infection clusters, we can see that the first infected individual becomes symptomatic just as they planned on travelling to a community center. Due to the 100% quarantine compliance, the infected individual stayed home until they recovered from their illness.[1] For the almost 100% infection clusters, we can see that the infected individual went to a community center the morning of Day 5 (1 day before symptom onset) and infected 2 other individuals. Because of this pre-symptomatic infection, the 2 other infected individuals manage to visit another community center before their symptom onset and thereby manage to start spreading the disease exponentially.

From this we can confirm that the 100% Quarantine compliance works as expected and quarantining individuals leads to more chances for the disease to stop spreading entirely.

5.2.5.3 Clustered Runs in relation to Infectivity

Looking at the experiments with an Exit Factor of 3 and 4 there are three clusters instead of the two clusters seen when given an Exit Factor of 5. In particular, the three clusters are approximately 0-20%, 33-40%, and 53-59%. The clusters were found by identifying sequences of runs more than 10% apart. Because of the larger drop for an Exit Factor of 3, we will focus on its clusters. In order to ensure statistical consistency, we ran these experiments an additional 40 times for a total of 50 times.

[1]For verification purposes, an example seed for this run is 8970356428476678143

Table 5.12: Clustered Runs given an Exit Factor of 3

40% Infectiousness

Cluster	Number of Runs
∼0-12%	19
∼33-39%	10
∼53-57%	21

50% Infectiousness

Cluster	Number of Runs
∼0-18%	25
∼37-43%	12
∼54-59%	13

Each cluster and the number of runs associated with the clusters can be seen in Table 5.12, where there is a noticeable difference in clustering depending on the Infectious Probability. In particular, for 40% infectiousness, we can see that $\frac{21}{50}$ runs infected 53-57% of the population while for 50% infectiousness, $\frac{25}{50}$ runs infected 0-18% of the population. Therefore, we now know why the average total infected population dropped even though the infectiousness of the disease increased. Furthermore, the cluster ranges are higher for higher infectiousness which falls in line with how a disease with a higher infection rate should behave.

Looking through a run which ends pre-maturely (37-43%) we find that in the beginning the infected population increases exponentially as infected individuals get lucky and spread the disease before quarantining measures take place. This can be seen in Figure 5.6 as both averages spike between Day 20 and Day 40. We note that even with a higher infectious rate, an Infectious Probability of 50% results in a lower and earlier spike in infections. This is a result of the higher infectious rate, which allows for lucky infected individuals to spread the disease more easily during pre-symptomatic infections. As a result of the quarantine strategy, we find that any increases in infected population depend heavily on pre-symptomatic individuals. However, as the infected population grows larger and the pool of susceptible individuals decreases, pre-symptomatic individuals come into less contact with individuals and are not able to infect as many new individuals. With a lack of new individuals to drive the pre-symptomatic infections, the infected population eventually dies out.

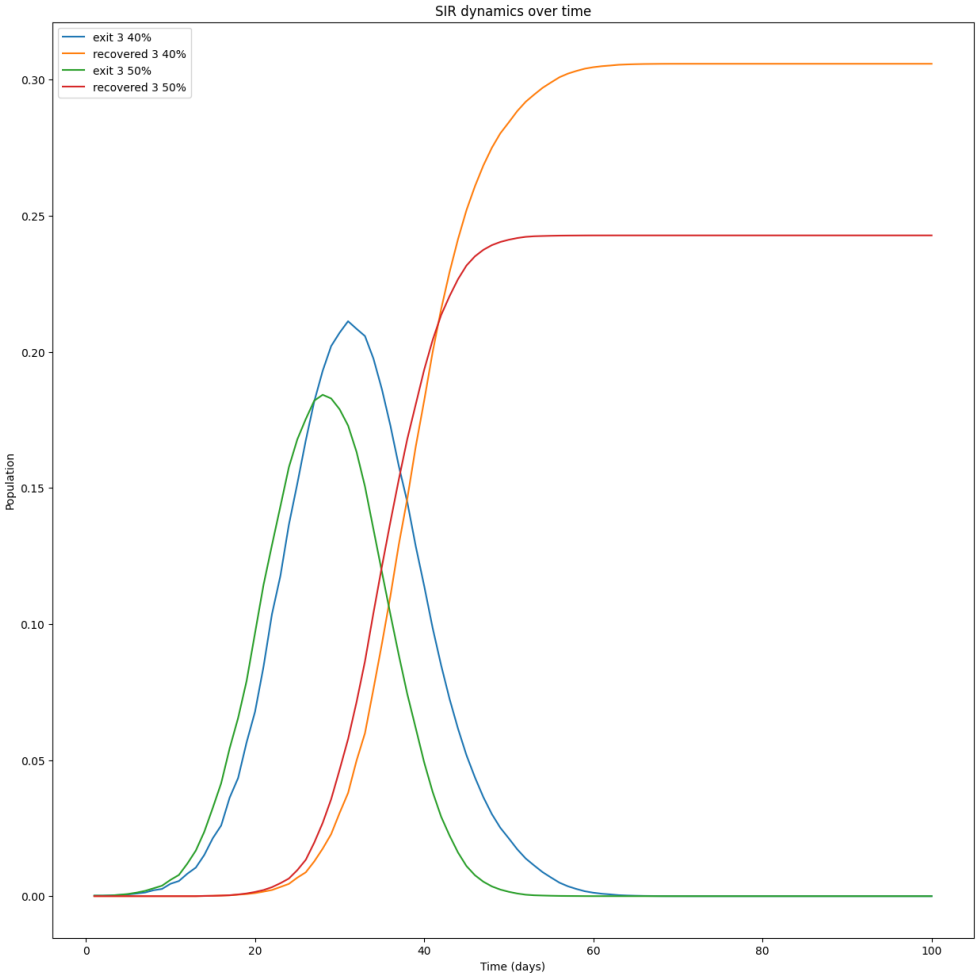

Figure 5.6: Average infected population for Exit 3 and Infectiousness 16% and 30%

We hypothesize that given a high enough infectious rate and 100% quarantine compliance, the disease may burn itself out by infecting too many individuals in the beginning of its spread which starves any future susceptible populations. This leads to a negative feedback loop that eventually wipes out the disease by itself.

Table 5.13: 90% and 80% Quarantine Compliance Average total infected population

	Infection Probability				
	90% Quarantine Compliance				
Exits	**0.16**	**0.2**	**0.3**	**0.4**	**0.5**
1	0.001	0.0	0.001	0.0	0.0
2	0.005	0.019	0.067	0.13	0.08
3	0.247	0.166	0.243	0.294	0.466
4	0.391	0.325	0.447	0.518	0.5
5	0.49	0.597	0.5	0.9	0.7

	80% Quarantine Compliance				
Exits	**0.16**	**0.2**	**0.3**	**0.4**	**0.5**
1	0.0	0.001	0.0	0.001	0.001
2	0.047	0.026	0.026	0.14	0.114
3	0.167	0.187	0.425	0.356	0.341
4	0.378	0.415	0.534	0.502	0.429
5	0.597	0.8	0.9	0.7	0.8

5.2.6 Variable Quarantine Strategies (90%, 80%)

Similar to Section 5.2.5, we find that at 40 and 50% Infectious probability, there is a drop in the average infected population. This may be due to the possible burnout hypothesized in Section 5.2.5.3.

To simplify comparisons, we approximated the range of infected populations across all Infectious Probabilities and filled out Table 5.14

Table 5.14: Comparison of approximate range for average infected population

	Quarantine Compliance		
Exits	**100%**	**90%**	**80%**
1	∼0-0.001	∼0-0.001	∼0-0.001
2	∼0.001-0.08	∼0.005-0.13	∼0.03-0.11
3	∼0.001-0.249	∼0.17-0.47	∼0.17-0.43
4	∼0.13-0.466	∼0.33-0.52	∼0.38-0.53
5	∼0.5-0.8	∼0.5-0.9	∼0.6-0.9

We can see that there is a great difference between 100% Quarantine compliance and 90/80% Quarantine compliance. In comparison with 100% Quarantine Compliance we find that the average infected population has increased as the quarantine compliance rate decreases. Looking only at an Infectious Probability of 16% and more significant infections, we find that even with an Exit Factor of 4, a 100% Quarantine compliance can lead to 13% of the population being infected. Surprisingly we also see that for

an Exit Factor of 3 but 80% Quarantine compliance, 17% of the population becomes infected.

In comparison with just using masks, Quarantine compliance has a much lower total infection rate. For these comparisons, we exclude Exit Factors 1 and 2 since all of the results resolve to around 0%. When comparing 100% Mask Usage with 100% Quarantine compliance, we find that at 16% Infectious probability, Quarantine compliance performs better with an almost 10% drop in infected individuals no matter the Exit Factor. At 20 and 30% Infectious probability, the drop in infected individuals is not as large but still significant.

5.2.7 Dependent Quarantine Strategies

One assumption we used for previous Quarantine strategies (Section 5.2.5) is that individuals quarantine independently of each other. We define dependent quarantining as households quarantining as one. Previously, individuals quarantined by themselves and it was possible for a household to have someone still traveling around but another member in quarantine. To see if quarantining as a household or quarantining as an individual has an effect on the infected population, we tested the same experiments in terms of Exit Factors and Infectious Probability. One important note for our dependent vs. independent strategy comparison is that because of our assumptions for individual traveling behaviors, dependent quarantining is aimed towards preventing the first infections in the pandemic. This is because of the assumption that only a single individual leaves the household, thus independent vs. dependent really only affects the first series of pre-symptomatic infections and thereby may not lead to large changes that we can expect from dependent quarantining.

5.2.7.1 100% Quarantine Compliance

Starting off with 100% Quarantine compliance, we can see the comparison in Table 5.15. The raw values for average total infected population can be seen in Table A.1 in the Appendix.

Table 5.15: Difference between Dependent 100% Quarantine and Independent 100% Quarantine

		Infection Probability				
		0.16	**0.2**	**0.3**	**0.4**	**0.5**
Exit Factor	**1**	-0.001	0.001	0	0.001	0.0
	2	0	-0.008	0.034	0.043	0.074
	3	0.054	-0.119	0.123	0.046	0.2
	4	0.059	0.068	0.025	0.201	-0.095
	5	0.08	0.003	-0.195	0.001	0.3

Overall for Exit Factors 1 and 2, there is almost 0 difference between independent and dependent quarantining. For Exit Factors 3 we can see a slight increase for 16% and 30% Infectiousness but a decrease for 20% Infectiousness. This means that when households quarantine as one, there was an increase of 5.4% individuals infected given an Infectious probability of 16%. Similarly there was a 11.9% decrease in infected individuals when the Infectious Probability was 20% and the Exit Factor was 3. Overall, for Exit Factors 4 and 5, the lower Infectious Probabilities (16% to 30%) are relatively stable with changes as high as 8% and as low as -20%.

The two largest changes were a 20% and 30% increase in infected individuals given large Infectious Probabilities (40-50%).

These results seem to indicate that overall for smaller Infectious Probabilities (16-30%), dependent quarantining can result in lower infection rates.

5.2.7.2 90% Quarantine Compliance

The raw results for the 90% Quarantine Compliance total infected population can be viewed in Table A.2 in the Appendix.

Table 5.16: Difference between Dependent 90% Quarantine and Independent 90% Quarantine

		Infection Probability				
		0.16	**0.2**	**0.3**	**0.4**	**0.5**
Exit Factor	**1**	-0.001	0.001	0	0.001	0.0
	2	-0.003	-0.007	0.006	0.027	0.003
	3	0.054	-0.007	0.045	0.059	-0.126
	4	-0.051	0.093	0.078	-0.132	-0.04
	5	0.099	0	0.499	-0.4	0.2

Similar to the previous section (Section 5.2.7.1), we see that for Exit Factors 1 and 2, the changes are almost 0%. For Exit Factors 3-5 and lower infectious rates (16% to 30%), almost every comparison has a low percentage change between -5% to 9.9%. However, the most noticeable is the 49.9% increase in infected individuals from household dependent quarantining. The logs detail that out of 10 runs for Exit Factor 5 and Infectious Probability 30%, $\frac{10}{10}$ runs infected 99-100% of the population. Similarly for Infectious probability 50%, where a 20% increase in infected individuals was noted. The logs recorded $\frac{9}{10}$ runs infecting 100% of the population while one run only infected 0.1%.

Besides the two outliers, most of the differences are in the realm of 10% or even lower, which suggests a minimal difference in dependent quarantining for 90% Quarantine compliance.

5.2.7.3 80% Quarantine Compliance

Similar to previous sections, the raw results for total infected population is visible in the Appendix at Table A.3

Table 5.17: Difference between Dependent 80% Quarantine and Independent 80% Quarantine

		Infection Probability				
		0.16	**0.2**	**0.3**	**0.4**	**0.5**
Exit Factor	**1**	0.0	0	0.001	-0.001	0
	2	-0.046	0.083	0.078	-0.03	-0.001
	3	0.1	0.096	-.126	-0.069	0.018
	4	0.016	-0.087	-0.217	-0.144	0.064
	5	-0.099	-0.1	-0.3	0	0.1

The comparison between 80% Dependent Quarantine and Independent 80% Quarantine can be seen in Table 5.17 with a much different result compared to previous comparisons. In this case almost all differences are less than 10% with many being negative (which means that dependent quarantining resulted in less infected individuals). In particular, we can see that for an Exit Factor of 4 and Infectious probability of 30%, dependent quarantining results in 21.7% less infected individuals on average.

Overall, we can see that having households quarantine as one results in minuscule effects to the infected population and even helps to reduce the number of infected in several cases.

5.2.8 Reverse Engineering R_0

To validate some of our results, we attempted to replicate current pandemic conditions and reverse engineer the Infectious Probability to closely approximate real-world R_0 values observed in California. To replicate current pandemic conditions, we varied quarantine compliance to 80% and mask usage to 80% and mainly focused on Infec-

tious Probabilities 10%, 16%, and 20%. Similar to previous experiments, we attempt both dependent and independent quarantining.

A quarantine compliance of 80% and mask usage of 80% was chosen to replicate the non-uniform compliance with intervention methods, a reasonable assumption is that if individuals will not comply with quarantine/mask interventions then they will not comply with mask/quarantine interventions. The Infectious Probabilities were limited to 10%, 16%, and 20% (with 10% being added specifically for this section) to replicate a more reasonable infectiousness since it has already been stated for 16% we assume close to worst case infectiousness [35].

5.2.8.1 Independent Quarantining

Table 5.18: Average R_0 for Independent Quarantine Compliance 80% and Mask Usage 80%

		Infection Probability		
		0.1	**0.16**	**0.2**
Exit Factor	**1**	0.35	0.684	0.444
	2	1.632	1.001	2.539
	3	1.397	4.86	2.066
	4	2.704	5.708	10.072
	5	4.663	9.044	10.827

As stated in Section 5.2.2.4, a cohort study found that secondary infections were estimated to be between 1.39 and 1.54 for Northern California and 2.06 to 2.49 for Southern California. Taking the 95% confidence interval for the whole of California, the range of secondary infections would then be from 1.14 to 3.33. Looking at our results in Table 5.18, we can see that for an Infectious Probability of 10%, Exit Factors 2 to 4 fall in line with the R_0 set by the cohort study. Other similar experiments include Infectious Probability 20% for Exit Factor 2 and 3.

5.2.8.2 Dependent Quarantining

Table 5.19: Average R_0 for Dependent Quarantine Compliance 80% and Mask Usage 80%

		Infection Probability		
		0.1	**0.16**	**0.2**
Exit Factor	**1**	0.434	0.556	0.926
	2	0.821	1.691	2.977
	3	0.991	4.051	3.734
	4	3.796	7.523	8.447
	5	2.857	7.352	13.07

The results that fall in the range of the cohort's study include Exit 2 16% Infectiousness, Exit 2 20% Infectiousness, and Exit 3 20% Infectiousness. While some of the other results do not fall into the 95% confidence interval listed by the cohort study, their R_0 values fall very close to the range. This includes results for all Exit Factors & Infectiousness of 10% and Exit Factors 1-3 for Infectiousness of 16% and 20%.

5.2.8.3 Validity

Ultimately for both dependent and independent quarantining, we find that for a reasonable infectious probability and intervention methods, we are able to replicate the R_0's found in real-world studies of Covid-19 spread throughout California. It is to be noted that R_0 is a highly location dependent measure as different communities can lead to unique interactions thereby affecting what the R_0 is. Taking this into account, this section is not a complete validation of our ABM's accuracy for predicting real-world epidemic dynamics in Cambria but does take a step towards it.

Chapter 6

SUMMARY AND FUTURE WORK

Over the course of this thesis, we have presented an Agent-Based Model (ABM) for simulating Covid-19 and applied to to the local community, Cambria Village. We simulated several scenarios:

1. Covid-19 spread without any interventions
2. Covid-19 spread with Mobility Restrictions
3. Covid-19 spread with Mobility Restrictions and variable Mask Usage
4. Covid-19 spread with Mobility Restrictions and variable Quarantine Compliance

6.1 Covid-19 spread without interventions

In this experiment, we mainly tested the capabilities of our ABM and to develop a base case to compare other experiments with. As expected, the disease infected approximately 100% of the population given no interventions and while varying the infectious probability.

6.2 Covid-19 spread with Mobility Restrictions

This experiment focused on restricting individuals' travel so that individuals could only travel 1-4 times a week. We found that leaving 4 times a week would on average infect 50-55% of the population. In comparison with our no intervention scenario of

exiting 5-7 times a week, which infected 100% of the population, we found a turning point between leaving 4 and 5 times a week that increased the infected population by 50%. Furthermore, the infected population did not follow with higher infectious rates, which led to a proposal that earlier spikes in infected populations could lead to a faster recovery spike and less infected individuals overall.

6.3 Covid-19 spread with Mobility Restrictions and variable Mask Usage

Building on our previous section with mobility restrictions, this experiment tested variable mask usage from 100-80% of the population wearing masks. At a 100% Mask Usage, the infected population was reduced but also in some cases the duration of the disease was extended past 100 days. We found that when the 80 to 90% of the population used masks, we started finding 2-3 clusters in our data. In comparison with our mobility restrictions results and no intervention results, mask usage was still useful in reducing the infected population.

6.4 Covid-19 spread with Mobility Restrictions and variable Quarantine Compliance

Our final experiment focused on implementing varying level of quarantine compliance. In particular, 80-100% of the population would quarantine when they start showing symptoms and we observed how that affected Covid-19 spread. One of the first discoveries was that similar to our Mask Usage experiment, we were experiencing clusters in our data. The clusters could be 2-3 clusters and we proposed a hypothesis on why these clusters came to be. In addition, we compared quarantining as a household and quarantining as an individual and found that quarantining as a household helped to reduce or cause no change in total infection levels for most lower infectious

rate cases. Overall, we found that complying with quarantine restrictions helped to reduce the spread of Covid-19 and would stop the virus within 100 days.

6.5 Future Work

As discussed in the previous sections, we have raised several interesting scenarios. The first was that given a high enough infectious rate and isolation strategies such as quarantine compliance or mask usage, a disease may burn itself out. This may be due to a lack of potential susceptible individuals or another undiscovered reason. Another scenario was in studying the turning point between leaving 4 and 5 times a week and why this caused such a large increase in infected individuals.

In addition, there are multiple extensions to this thesis that can be done. In particular, simulating contact tracing, age-based networks, and additional community centers like workplaces and schools would be beneficial to better understanding the spread of Covid-19.

Finally, our model can be better fine tuned for local communities. To better understand unique mobility restrictions we could survey the population of Cambria to get a better understanding of the community's mobility dynamics. In particular, we could stop using our assumptions and start using empirical observations of real-world dynamics.

Chapter 7

LIMITATIONS

7.1 Agent-Based Models

Although agent-based models enable a more bottom-up approach in studying individuals and populations during infectious diseases, there are certain limitations associated with agent-based models that apply to our implemented model. As a stochastic model, ABMs have an innate uncertainty associated with it and adding different tuning factors in the simulation can lead to increased uncertainty [19]. Our approach for the ABM works backwards by defining relationships to create the model instead of using empirical real-life data to define model parameters. As a result verification of results can only be relegated to a comparison of epidemic parameters with the COVID-19 pandemic and cannot completely verify the accuracy of the model.

7.2 Assumptions

As part of the consequence of using a bottom-up approach, much of our model is founded on assumptions about human nature and their behavioral patterns. In order to capture the mobility of individuals during a pandemic, we had to make assumptions about how often individuals leave their household and who is allowed to leave the household. Furthermore, assumptions such as the number of community centers are very dependent on the specific use case. For instance, in our case study of Cambria, we personally looked at the grocery stores and decided to use two as the community centers in our model. Finally, assumptions about the disease are from

recently published papers that may not have had time to pass a stringent peer review due to the international push for study of the Covid-19 virus. Therefore, it is possible for assumptions about disease parameters such as infectiousness, viral load, and incubation period to be incorrect.

7.3 Validation of Results

An important part of epidemiological studies is the validation of results. Many of our related works validate their models by comparing their models' results with real-world data from the Covid-19 pandemic [18] [13] [46] [41]. In our case, our ABM was created using just the community's census numbers such as the population, mean population per household, and the number of households. Everything else about our epidemic model such as the infectiousness, mask infectiousness reduction, etc. are second-hand data from other researchers and allowed to vary [35] [17]. Because of this, our model allows for flexible experimentation but the wide assumptions results in non-specific data that cannot be compared to real-world data as other epidemiological studies have done. As a result, our model is limited to more general comparisons such as the infected population and its dynamics over time. We provide a step towards validity in Section 5.2.8 by validating that we can reach similar R_0s found in real-world data.

Chapter 8

CONCLUSION

This thesis presented an Agent-Based Model (ABM) built on Python that was able to simulate Covid-19 spread over a local community. We were able to simulate various scenarios for intervention and prevention of disease spreading and observed its effect on the amount of infected individuals. In particular, we found that quarantining as a household, using masks, and restricting travel outside of households less than or equal to 4 times a week was helpful in reducing the number of infected individuals. In addition, we proposed future work that could help expand upon our ABM and make our model more accurate for local communities.

BIBLIOGRAPHY

[1] Cal Poly Github. http://www.github.com/CalPoly.

[2] WHO Director-General's opening remarks at the media briefing on COVID-19. https://www.who.int/director-general/speeches/detail/who-director-general-s-opening-remarks-at-the-media-briefing-on-covid-19---11-march-2020, Mar 2020.

[3] H. ABBEY. An examination of the reed-frost theory of epidemics. *Human biology*, 24(3):201..233, September 1952.

[4] O. M. Araz, J. W. Fowler, T. W. Lant, and M. Jehn. A pandemic influenza simulation model for preparedness planning. In *Proceedings of the 2009 Winter Simulation Conference (WSC)*, pages 1986–1995, 2009.

[5] A. Arenas, W. Cota, J. Gómez-Gardeñes, S. Gómez, C. Granell, J. T. Matamalas, D. Soriano, and B. Steinegger. *A mathematical model for the spatiotemporal epidemic spreading of COVID19*. Mar 2020.

[6] J. T. Brooks and J. C. Butler. Effectiveness of Mask Wearing to Control Community Spread of SARS-CoV-2. *JAMA*, 325(10):998–999, 03 2021.

[7] U. S. C. Bureau. Quickfacts Cambria CDP, california. https://www.census.gov/quickfacts/cambriacdpcalifornia, Jan 2019.

[8] Centers for Disease Control and Prevention. Severe Acute Respiratory Syndrome (SARS). https://www.cdc.gov/sars/index.html, 2017.

[9] Centers for Disease Control and Prevention. Cdc Human Coronavirus Types: Information about the six types of coronaviruses including MERS-CoV and SARS-CoV. https://www.cdc.gov/coronavirus/types.html, Mar 2021.

[10] M. Cevik, J. L. Marcus, C. Buckee, and T. C. Smith. Severe acute respiratory syndrome coronavirus 2 (sars-cov-2) transmission dynamics should inform policy. *Clinical Infectious Diseases*, page ciaa1442, Sep 2020.

[11] M. Cevik, M. Tate, O. Lloyd, A. E. Maraolo, J. Schafers, and A. Ho. Sars-cov-2, sars-cov, and mers-cov viral load dynamics, duration of viral shedding, and infectiousness: a systematic review and meta-analysis. *The Lancet Microbe*, 2(1):e13–e22, Jan 2021.

[12] S. Chen and C. Lanzas. Distinction and connection between contact network, social network, and disease transmission network. *Preventive Veterinary Medicine*, 131:8–11, Sep 2016.

[13] N. N. Chung and L. Y. Chew. *Modelling Singapore COVID-19 pandemic with a SEIR multiplex network model*. Jun 2020.

[14] S. L. O. County. Current Emergency Information. https://www.emergencyslo.org/en/positive-case-details.aspx, 2021.

[15] D. J. Daley and J. Gani. *Epidemic Modelling an Introduction*. Cambridge University Press, 1999.

[16] V. J. Davey and R. J. Glass. Rescinding community mitigation strategies in an influenza pandemic. *Emerging Infectious Diseases*, 14(3):365–372, Mar 2008.

[17] P. Doung-ngern, R. Suphanchaimat, A. Panjangampatthana, C. Janekrongtham, D. Ruampoom, N. Daochaeng, N. Eungkanit,

N. Pisitpayat, N. Srisong, O. Yasopa, and et al. Case-control study of use of personal protective measures and risk for sars-cov 2 infection, thailand. *Emerging Infectious Diseases*, 26(11):2607–2616, Nov 2020.

[18] S. E. Eikenberry, M. Mancuso, E. Iboi, T. Phan, K. Eikenberry, Y. Kuang, E. Kostelich, and A. B. Gumel. To mask or not to mask: Modeling the potential for face mask use by the general public to curtail the covid-19 pandemic. *Infectious Disease Modelling*, 5:293–308, 2020.

[19] A. El-Sayed, P. Scarborough, L. Seemann, and S. Galea. Social network analysis and agent-based modeling in social epidemiology. *Epidemiologic perspectives & innovations : EP+I*, 9:1, 02 2012.

[20] J. M. Epstein and R. Axtell. *Growing artificial societies: social science from the bottom up.* Brookings Institution Press, 1996.

[21] O. Fielding. A History of Rabies. https://www.tuckahoevet.com/post/a-history-of-rabies.

[22] V. Gemmetto, A. Barrat, and C. Cattuto. Mitigation of infectious disease at school: targeted class closure vs school closure. *BMC Infectious Diseases*, 14(1):695, Dec 2014.

[23] C. Granell and P. J. Mucha. Epidemic spreading in localized environments with recurrent mobility patterns. *Physical Review E*, 97(5):052302, May 2018.

[24] M. H. Haischer, R. Beilfuss, M. R. Hart, L. Opielinski, D. Wrucke, G. Zirgaitis, T. D. Uhrich, and S. K. Hunter. Who is wearing a mask? gender-, age-, and location-related differences during the covid-19 pandemic. *PLOS ONE*, 15(10):e0240785, Oct 2020.

[25] H. W. Hethcote. The mathematics of infectious diseases. *SIAM Review*, 42(4):599–653, Jan 2000.

[26] N. Hoertel, M. Blachier, C. Blanco, M. Olfson, M. Massetti, M. S. Rico, F. Limosin, and H. Leleu. A stochastic agent-based model of the SARS-CoV-2 epidemic in France. *Nature Medicine*, 26(9):1417–1421, Sept. 2020.

[27] B. Jarosz. Poisson distribution: A model for estimating households by household size. *Population Research and Policy Review*, 40(2):149–162, Apr 2021.

[28] J. H. Jones. Notes On R_0. https://web.stanford.edu/~jhj1/teachingdocs/Jones-on-R0.pdf, 2007. Accessed: 4-27-2021.

[29] C. Kantis, S. Kiernan, and J. Bardi. Updated: Timeline of the Coronavirus. https://www.thinkglobalhealth.org/article/updated-timeline-coronavirus, 2021.

[30] W. O. Kermack and A. G. McKendrick. A contribution to the mathematical theory of epidemics. *Proceedings of the royal society of london. Series A, Containing papers of a mathematical and physical character*, 115(772):700–721, 1927.

[31] P. Klepac, A. J. Kucharski, A. J. Conlan, S. Kissler, M. L. Tang, H. Fry, and J. R. Gog. *Contacts in context: large-scale setting-specific social mixing matrices from the BBC Pandemic project*. Feb 2020.

[32] A. J. Kucharski, P. Klepac, A. J. K. Conlan, S. M. Kissler, M. L. Tang, H. Fry, J. R. Gog, W. J. Edmunds, J. C. Emery, G. Medley, and et al. Effectiveness

of isolation, testing, contact tracing, and physical distancing on reducing transmission of sars-cov-2 in different settings: a mathematical modelling study. *The Lancet Infectious Diseases*, 20(10):1151–1160, Oct 2020.

[33] N. Lanese. What is a coronavirus? https://www.livescience.com/what-are-coronaviruses.html, 2020.

[34] J. A. Lewnard, V. X. Liu, M. L. Jackson, M. A. Schmidt, B. L. Jewell, J. P. Flores, C. Jentz, G. R. Northrup, A. Mahmud, A. L. Reingold, M. Petersen, N. P. Jewell, S. Young, and J. Bellows. Incidence, clinical outcomes, and transmission dynamics of severe coronavirus disease 2019 in california and washington: prospective cohort study. *BMJ*, 369, 2020.

[35] Z. J. Madewell, Y. Yang, I. M. Longini, M. E. Halloran, and N. E. Dean. Household transmission of sars-cov-2: A systematic review and meta-analysis. *JAMA Network Open*, 3(12):e2031756, Dec 2020.

[36] Merriam-Webster. Pandemic. In *Merriam-Webster.com dictionary*.

[37] B. News. Covid-19: First Vaccine given in US as roll-out begins. *BBC News*, Dec 2020.

[38] W. H. Organization. Pneumonia of unknown cause – China. https://www.who.int/csr/don/05-january-2020-pneumonia-of-unkown-cause-china/en/, Jan 2020.

[39] J. Parker and J. Epstein. A distributed platform for global-scale agent-based models of disease transmission. *ACM transactions on modeling and computer simulation : a publication of the Association for Computing Machinery*, 22:2, 12 2011.

[40] Poutanen, Susan M. . Human Coronavirus 229e. https://www.sciencedirect.com/topics/neuroscience/human-coronavirus-229e, 2018.

[41] R. J. Rockett, A. Arnott, C. Lam, R. Sadsad, V. Timms, K.-A. Gray, J.-S. Eden, S. Chang, M. Gall, J. Draper, and et al. Revealing covid-19 transmission in australia by sars-cov-2 genome sequencing and agent-based modeling. *Nature Medicine*, 26(9):1398–1404, Sep 2020.

[42] P. Sapiezynski, A. Stopczynski, D. D. Lassen, and S. Lehmann. Interaction data from the copenhagen networks study. *Scientific Data*, 6(1):315, Dec 2019.

[43] K. Sasaki. Covid-19 dynamics with sir model. http://www.lewuathe.com/covid-19-dynamics-with-sir-model.html, Mar 2020.

[44] L. Sauer. What is coronavirus? https://www.hopkinsmedicine.org/health/conditions-and-diseases/coronavirus, 2021.

[45] A. Scala, A. Flori, A. Spelta, E. Brugnoli, M. Cinelli, W. Quattrociocchi, and F. Pammolli. Time, space and social interactions: exit mechanisms for the covid-19 epidemics. *Scientific Reports*, 10(1), Aug 2020.

[46] M. Small and D. Cavanagh. Modelling strong control measures for epidemic propagation with networks—a covid-19 case study. *IEEE Access*, 8:109719–109731, 2020.

[47] M. Tracy, M. Cerdá, and K. M. Keyes. Agent-based modeling in public health: Current applications and future directions. *Annual Review of Public Health*, 39(1):77–94, Apr 2018.

[48] A. L. Ziff and R. M. Ziff. Fractal kinetics of covid-19 pandemic. *medRxiv*, 2020.

APPENDICES

Appendix A

ADDITIONAL EXPERIMENTAL RESULTS

A.1 SIR Dynamics of Exit Factor 6 and Infectious Probability 0.2

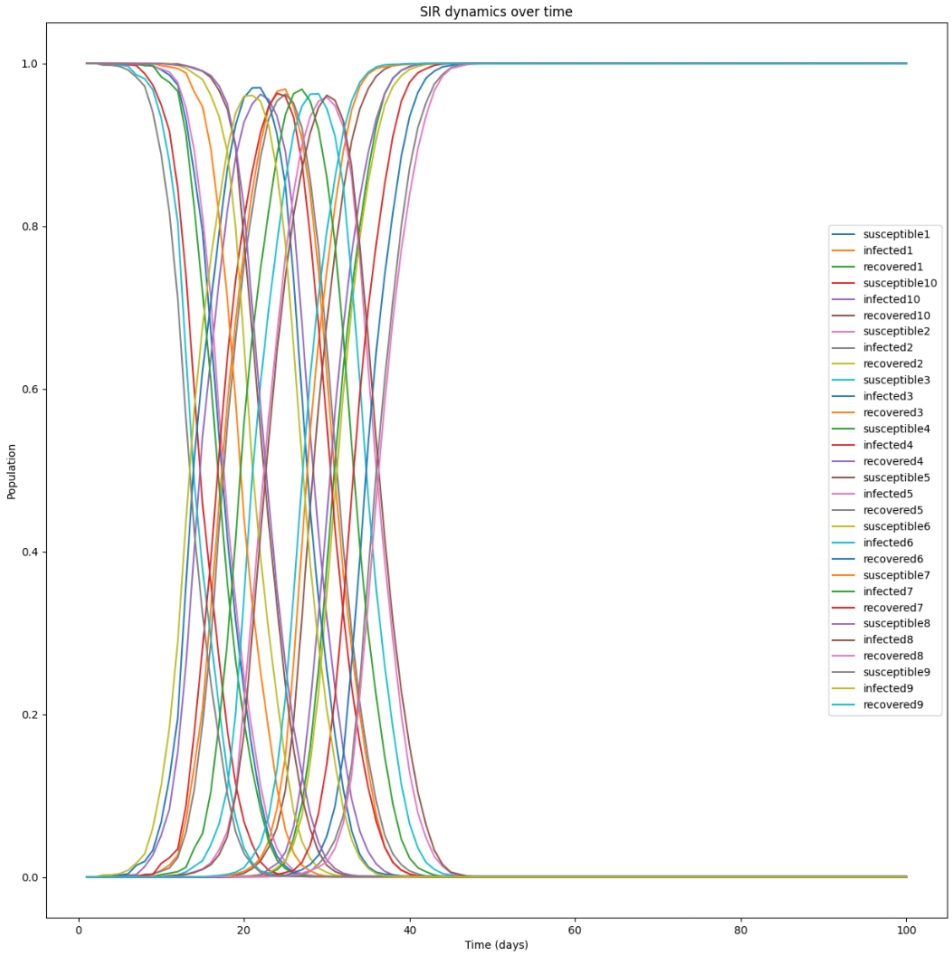

Figure A.1: SIR Dynamics of Exit Factor 6 and Infectious Probability 0.2

A.2 100% Quarantine compliance average total infected population when households quarantine together

Raw data for total average infected population when households quarantine together and 100% Quarantine compliance.

Exit Factor \ Infection Probability	**0.16**	**0.2**	**0.3**	**0.4**	**0.5**
1	0.0	0.001	0.001	0.001	0.0
2	0.001	0.001	0.035	0.089	0.15
3	0.055	0.002	0.361	0.364	0.449
4	0.189	0.38	0.393	0.511	0.371
5	0.605	0.752	0.595	0.699	0.8

Table A.1: 100% Quarantine compliance average total infected population

A.3 90% Quarantine compliance average total infected population when households quarantine together

Raw data for total average infected population when households quarantine together and 90% Quarantine compliance.

Exit Factor \ Infection Probability	**0.16**	**0.2**	**0.3**	**0.4**	**0.5**
1	0.0	0.001	0.001	0.001	0.0
2	0.002	0.012	0.073	0.157	0.083
3	0.301	0.159	0.288	0.353	0.34
4	0.34	0.418	0.525	0.386	0.46
5	0.589	0.597	0.999	0.5	0.9

Table A.2: 90% Quarantine compliance average total infected population

A.4 80% Quarantine compliance average total infected population when households quarantine together

Raw data for total average infected population when households quarantine together and 80% Quarantine compliance.

Exit Factor \ Infection Probability	**0.16**	**0.2**	**0.3**	**0.4**	**0.5**
1	0.0	0.001	0.001	0.0	0.001
2	0.001	0.109	0.104	0.11	0.113
3	0.267	0.283	0.299	0.287	0.359
4	0.394	0.328	0.317	0.358	0.493
5	0.498	0.7	0.6	0.7	0.9

Table A.3: 80% Quarantine compliance average total infected population

Appendix B

ADDITIONAL INFORMATION

B.1 Empirical Data on effects of Covid-19 on Cambria

Data for the total amount of infections can be found in the San Luis Obispo County Covid-19 dashboard [14]. As of June 2021, Cambria has had 185 cases of Covid-19. A graph of the total infected population from June 2020 to around May 2020 can be seen in Figure B.1. The spike in infections corresponds with the spike in overall infections nationwide around January of 2021. Overall, Cambria has done well against the infection with such a low total infected population. Unfortunately, we are not able to see a delineation of cases by age group but the SLO Covid-19 dashboard does provide information about the county's cases delineated by age.

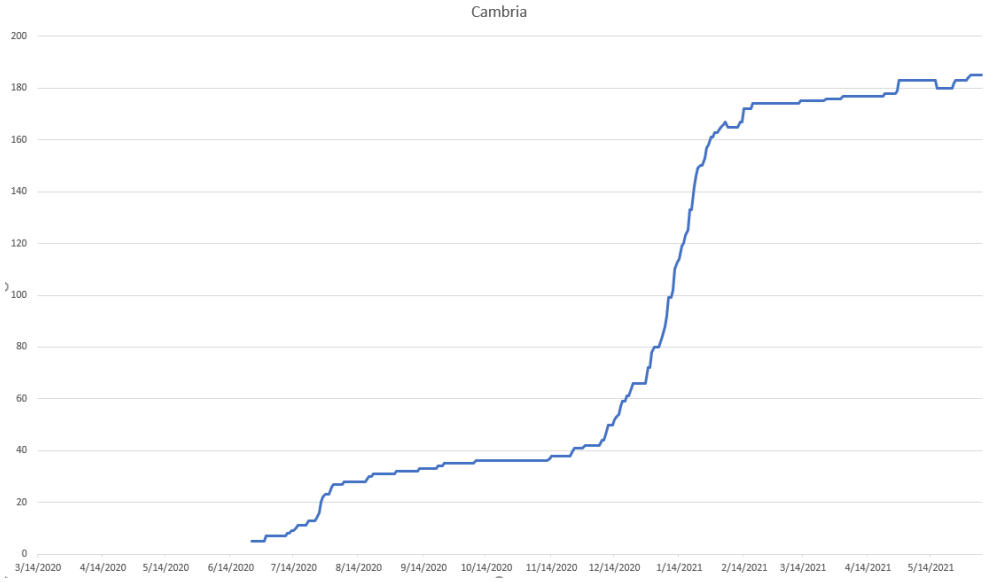

Figure B.1: Total infected population over time for Cambria